Electronic Supplementary Material (ESI) for RSC Advances.

Supporting information for the manuscript entitled *Synthesis, Characterisation and Functionalisation of BAB-type Dual-Responsive Nanocarriers for Targeted Drug Delivery: Evolution of Nanoparticles based on 2-Vinylpyridine and Diethyl Vinylphosphonate*

Andreas Saurwein,[‡a] Andreas Schaffer,[‡a] Christina Wieser,[a] and Bernhard Rieger[*a]

[a]WACKER-Chair of Macromolecular Chemistry, Catalysis Research Center, Technical University of Munich, Lichtenbergstraße 4, 85747 Garching near Munich, Germany. E-mail: rieger@tum.de.

Contents

1 Materials and Methods

General Information

All moisture- or air-sensitive reactions were carried out under argon atmosphere using standard Schlenk technique or a glovebox. All glassware was heat dried under vacuum prior to use. Unless otherwise stated, all chemicals were purchased from *Sigma-Aldrich* or *TCI Chemicals* and used as received. Toluene were dried using a *MBraun* SPS-800 solvent purification system and stored of 3 Å molecular sieve. $Cp_2Y(THF)(CH_2TMS)$ (**4**)[1-4], $Cp_2Y(CH_2(C_5H_2Me_2N))$[5], diethyl vinylphosphonate (DEVP)[6] and diallyl vinylphosphonate (DAlVP)[7, 8] were prepared according to procedures found in the literature. The monomers 2-vinylpyridine (2VP), DEVP, and DAlVP were dried over calcium hydride and distilled prior to use. The folate-NHS active ester was synthesised according to a published procedure.[9, 10]

Dialysis

Purification of products via diaysis were rendered with *Spectra/Por 1* dialysis membranes (regenerated cellulose) from *VWR* against deionized water. The membranes used have a molecular weight cut-off of (MWCO) of 6-8 kDa and 3.3 mL cm^{-1} volume-length ratio. Loading and release experiments of the nanoparticles were rendered with *ZelluTrans T2* dialysis membranes (regenerated cellulose) from *Carl Roth*. These membranes have a molecular weight cut-off of (MWCO) of 6-8 kDa and 0.32 mL cm^{-1} volume-length ratio Prior to use the membranes were treated with deionized water over night.

Dynamic Light Scattering (DLS)

Hydrodynamic diameters of the particles were determined on a *Zetasizer Nona ZS* from *Malvern*. The samples were dissolved in *Millipore* water or HPLC chloroform at a concentration of 2.5 mg mL^{-1}. The DLS data were averaged from three measurements which for their part consisted of eleven single measurements.

Gel Permeation Chromatography (GPC)

For the determination of the molecular weight distributions polymer solutions with a concentration of 2.5 mg mL^{-1} were conducted to GPC measurements on a *PL-GPC 50* with two PL-Gel columns from *Agilent Technologies.* DMF with 2.17 g L^{-1} lithium bromide as additive was used as eluent. Absolute molar masses were determined *via* an integrated dual-angle light scattering detector and a RI detection unit for concentration calculation.

Elemental Analysis (EA)

Elemental analyses were performed on a *Vario EL* from *Elemetar* at the microanalytical lab of the inorganic-chemical institute at the Technical University Munich (TUM).

UV/Vis Spectroscopy

UV/vis spectra were recorded on a *Cary 50* UV/vis spectrophotometer from *Varian*. For the measurements quartz glass cuvettes were filled with samples dissolved in deionized water or methanol.

Photoluminescence Spectroscopy (PL)

Photoluminescence measurements were performed on *AVA-Spec 2048* from *Avantes*. For the excitation of the samples PS cuvettes were placed in a 90° cuvette holder consisting of *Prizmatix* current controller as light source irradiated with light of a wavelength of 365 nm.

Nuclear Magnetic Resonance Spectroscopy (NMR)

Nuclear magnetic resonance spectra were recorded on the devices *AVIII 300* (300 MHz), *AVIII 400 HD* (400 MHz) and a *AVIII 500 cryo* (500 MHz) from *Bruker*. Deuterated solvents were purchased from *Sigma-Aldrich*. For moisture-sensitive purposes the solvents were dried over 3 Å molecular sieve. ^{1}H and ^{13}C spectroscopic chemical shifts δ are reported in ppm and calibrated to the residual proton signals of the used solvents.

Benzene-d_6: δ (ppm) = 7.16 (^{1}H NMR); δ (ppm) = 128.1 (^{13}C NMR).

Dimethyl sulfoxide-d_6: δ (ppm) = 2.50 (^{1}H NMR); δ (ppm) = 39.5 (^{13}C NMR).

Methanol-d_4: δ (ppm) = 4.87 (^{1}H NMR); δ (ppm) = 49.0 (^{13}C NMR).

Unless otherwise stated coupling constants *J* are mean values and refer to coupling between two protons. For the assignment of the signals the signal multiplicities were abbreviated accordingly: s – singlet, d – doublet, t – triplet, m – multiplet.

Transmission Electron Microscopy (TEM)

Imaging via TEM was rendered with *JEM-1400 Plus* from *JEOL* with a magnification factor of 6 x 10^4. The *LaB6* filament was operated with an acceleration voltage of 120 kV. Aqueous nanoparticle solutions (2.5 mg mL^{-1}) were adsorbed on copper grid with a continuous film of charcoal for one minute and subsequently stained with uranylacetate (2 wt-%) solution. TEM images were used to determine an average diameter, a standard deviation and the polydispersity from 60 particles.

Turbidity Measurements

The determination of the cloud point was carried out on Cary *50* UV/vis spectrophotometer from *Varian* in 4 mL glass cuvettes using a peltier thermostat. Polymer or Nanoparticle solutions with a concentration of 2.5 mg mL^{-1} were used and heated/cooled with a rate of 1 K min^{-1} followed by a five-minute-long waiting period to establish a thermal equilibrium. The cloud point was detected by the changes in transmittance at λ = 500 nm. The lower critical solution temperature was defined as the temperature corresponding to a decrease of 10% in optical transmittance.

Zeta Potential Measurements

Zeta potentials ζ were measured on a *Zetasizer Nano ZS* from *Malvern* using aqueous solutions of the nanoparticles (2.5 mg mL^{-1}) and averaged from three measured values.

Loading of the Nanoparticles

For loading with fluorescein a solution of 6.96 mg nanoparticles was dissolved in 1.66 mL deionized water to adjust a concentration of 4.2 g mL^{-1}. To this solution a solution of fluorescein (580 mg) in DMSO (1.94 mL) was added dropwise at 0 °C. After stirring for 45 minutes at this temperature the mixture was stirred for additional 90 minutes at room temperature. Subsequently five dialysis membranes were filled with 600 µL each of this

solution and were dialysed against deionized water (500 mL) over night. Likewise, a sixth tubing was filled with 600 µL of the solution and dialysed against 100 mL deionized water over night. 1.5 mL were taken from the medium of the sixth dialysis and conducted to a photoluminescence measurement to obtain a reference value for the already released fluorescein.

Release Experiments

For the release studies the five dialysis tubes were placed in the corresponding media (60 mL) (deionized water for temperature-related measurements and citrate-buffer solutions with a pH of 4.5 or 6.0). Samples (1.5 mL) were taken at regular intervals (hourly during the first 7 hours, then after 24, 30, 48 and 72 hours) and the removed volume was backfilled with 1.5 mL of the related medium. Each sample taken was later conducted to photoluminescence spectroscopy. The amount of fluorescein was then determined from the relative irradiance at each measuring point using calibration curves. The calibration curves were generated *via* photoluminescence measurements using fluorescein solutions in water and the citrate-buffer solutions with varying concentrations. With help of the reference sample (*vide infra*, initial amount of fluorescein) the fraction of released fluorescein was calculated.

2 Complex Synthesis

C-H bond activation of TMPy (1) with $Cp_2Y(CH_2TMS)(THF)$ (4)

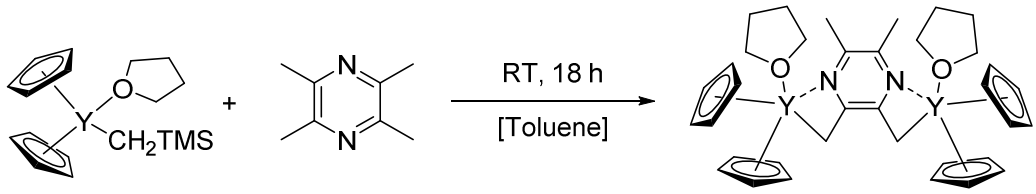

4 $C_{18}H_{29}OSiY$ 378.42 g/mol

1 $C_8H_{12}N_2$ 136.20 g/mol

5 $C_{36}H_{46}N_2O_2Y_2$ 716.59 g/mol

Complex **4** (83.4 mg, 220 µmol, 2.0 equiv.) was dissolved in absolute toluene (3.0 mL). 2,3,5,6-Tetramethylpyrazine (**1**) (15.0 mg, 110 µmol, 1.0 equiv.) was dissolved in absolute toluene (1.5 mL), added to the complex solution and rinsed with another 1.5 mL of dry toluene. Immediately after addition of the initiator a deeply orange solution could be observed. After four hours full conversion was detected *via* ^{1}H-NMR spectroscopy. Hereafter the solvent was removed under reduced pressure and the residue was washed with pentane. The supernatant solution was decanted of and the solid dried in high vacuum to afford complex **5** (84 %, 66.5 mg,92.8 µmol) as a red powder.

^{1}H NMR (500 MHz, Benzene-d_6, 300 K): δ (ppm) = 6.11 (s, 20H, Cp), 3.50 – 3.36 (m, 8H, THF), 2.91 (s, 4H, CH_2Y), 1.99 (s, 6H, CH_3), 1.35 – 1.17 (m, 8H, THF).

^{13}C NMR (126 MHz, Benzene-d_6, 300 K): δ (ppm) = 153.3 (s, $C_{Pyrazine}$), 127.2 (s, $C_{Pyrazine}$), 111.0 (d, Cp), 69.9 (t, THF), 45.5 (dt, J_{CY} = 5.0 Hz, CH_2Y), 25.6 (t, THF), 19.4 (q, CH_3).

EA: calculated: C 60.34 H 6.47 N 3.91
found: C 59.29 H 6.31 N 3.86

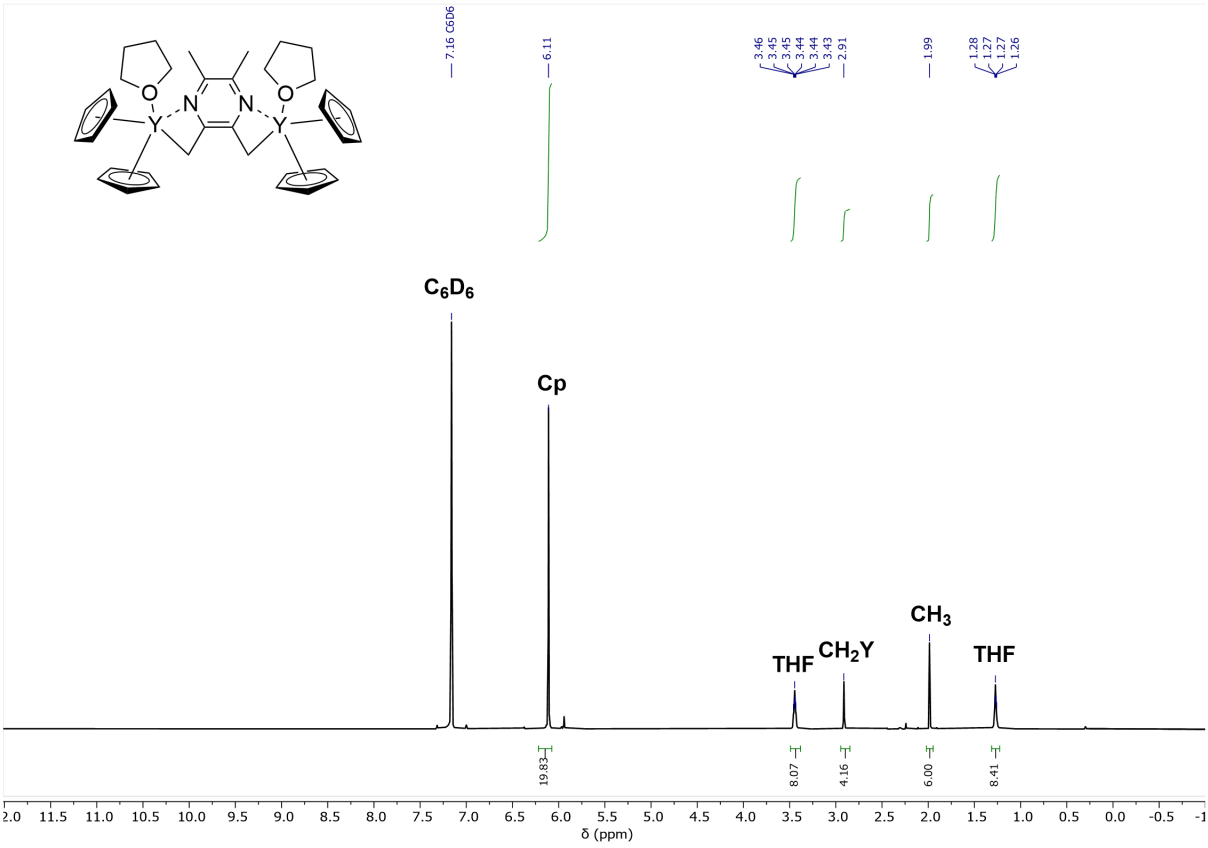

Fig. S1 ^{1}H-NMR spectrum of complex **5** recorded in benzene-d_6.

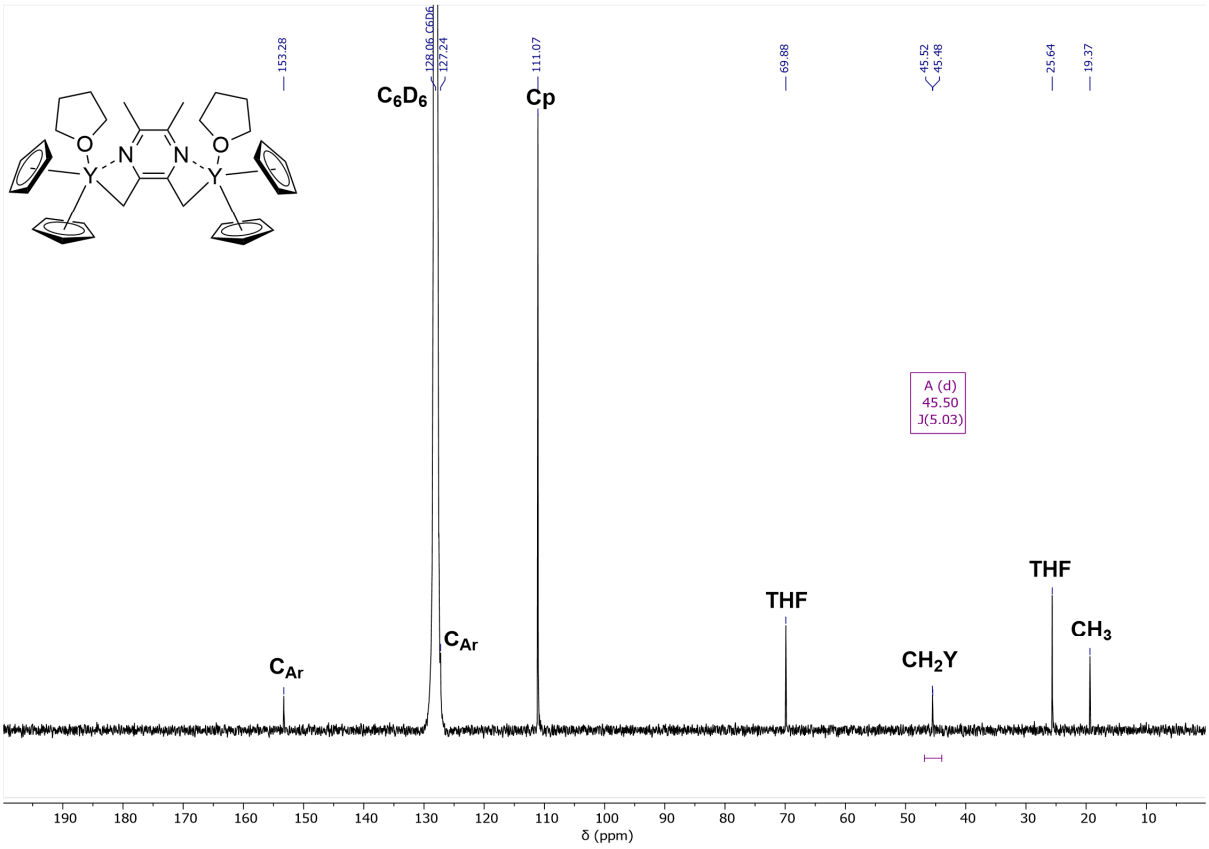

Fig. S2 ^{13}C-NMR spectrum of complex **5** recorded in benzene-d_6.

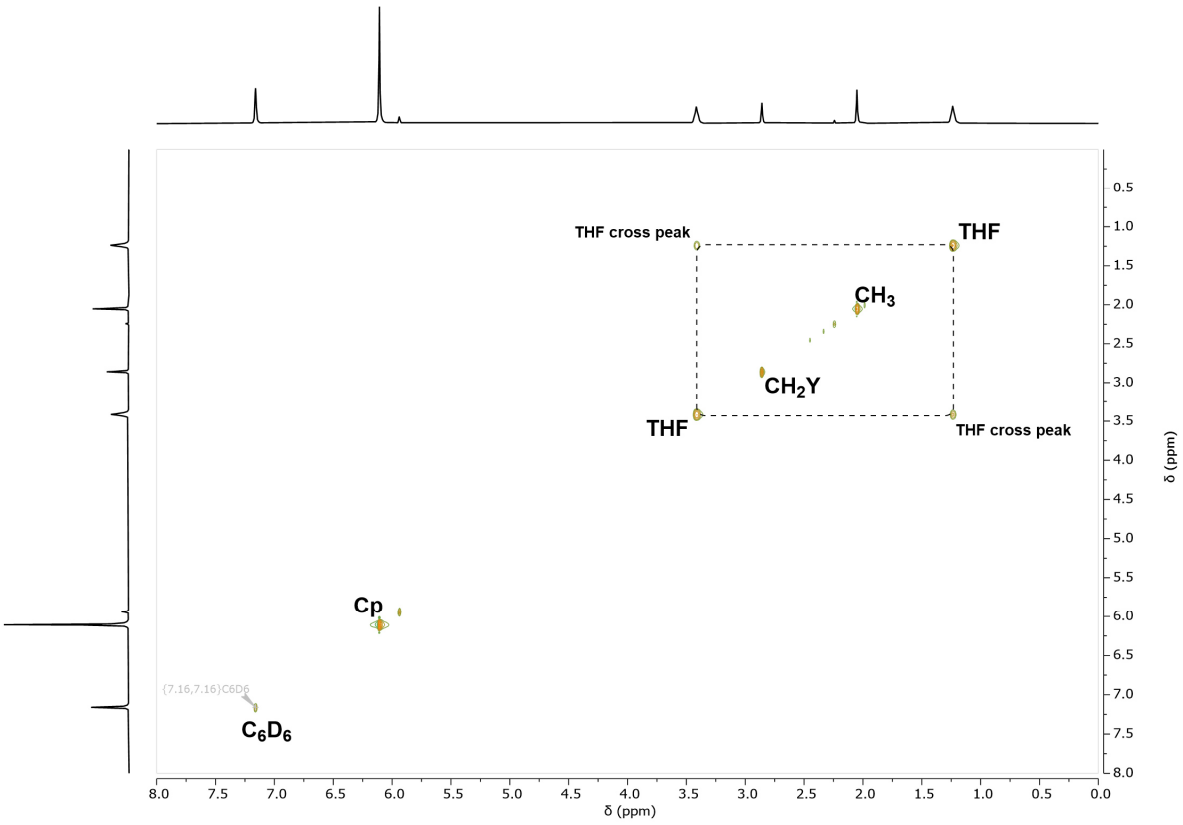

Fig. S3 NOESY spectrum of complex **5** recorded in benzene-d_6.

Kinetic investigation of the C-H bond activation of 2,3,5,6-Tetramethylpyrazine (1)

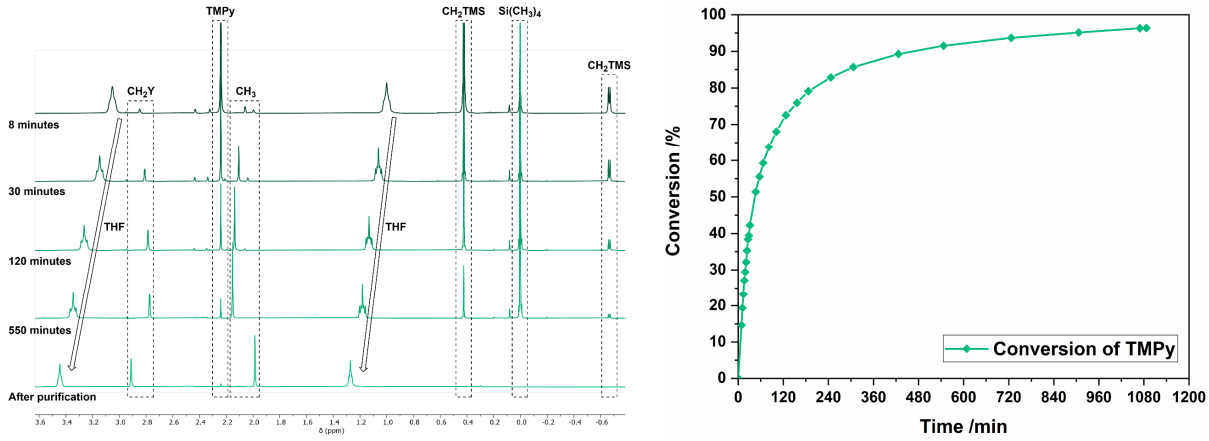

Fig. S4 Selected ^{1}H-NMR spectra of the kinetic analysis of the C-H bond activation of TMPy (**1**) recorded in benzene-d_6 (left) and time-dependent plot of the calculated conversions (right).

Oligomerization with 2,3,5,6-tetramethylpyrazine and *sym*-collidine

A solution of $Cp_2Y(CH_2TMS)(THF)$ (**4**) (46.1 mg, 122 µmol, 2.00 equiv.) in absolute toluene (1.00 mL) was added to 2,3,5,6-tetramethylpyrazine (**1**) (8.29 mg, 60.9 µmol, 1.00 equiv.) in absolute toluene (1.00 mL) and resulted in the instant colouring of the reaction mixture. After the quantitative conversion was detected by ^{1}H-NMR spectroscopy, the mixture was diluted with 3.00 mL of toluene, and 2-vinylpyridine (64.0 mg, 609 µmol, 5.00 equiv.) was added in one portion. After 20 hours proton NMR confirmed the complete conversion of 2-vinylpyridine. The oligomerisation was terminated by addition of methanol and precipitated in pentane. The supernatant phase was decanted off and the oligomer was dried in vacuum. For the analysis by ESI-MS the oligomer was dissolved in LC-MS methanol at concentration of 0.10 mg mL^{-1}.

The oligomerisation of 2-vinylpyridine with *sym*-collidine as initiator was performed with a reduced amount of complex **4** (23.1 mg, 60.9 µmol, 1.00 equiv.).

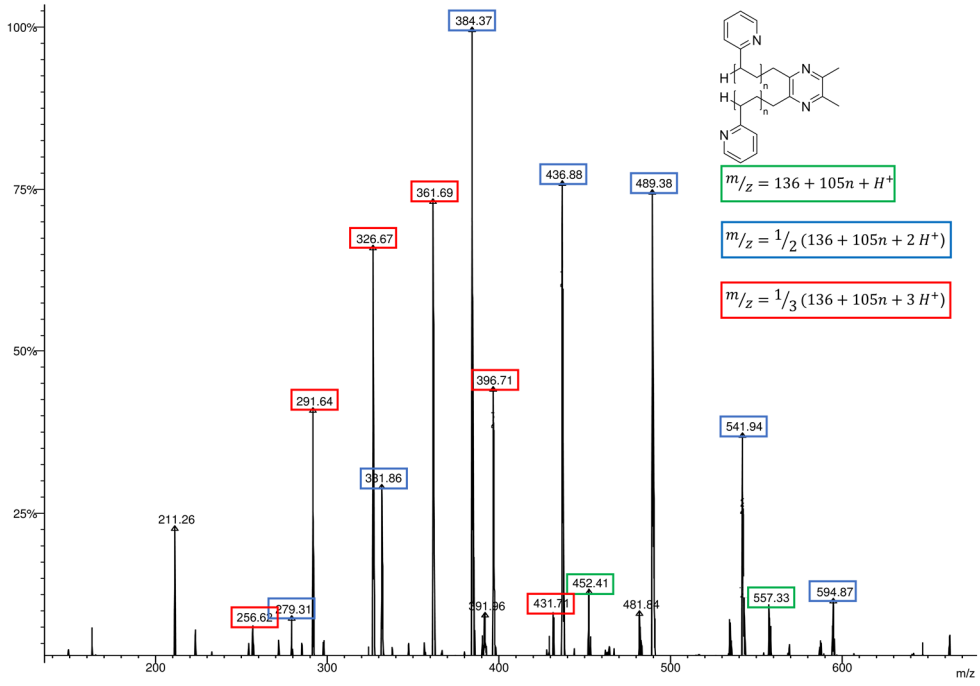

Fig. S5 ESI-MS spectrum of 2VP oligomers generated with complex **4** and 2,3,5,6-tetramethylpyrazine (**1**) as initiator.

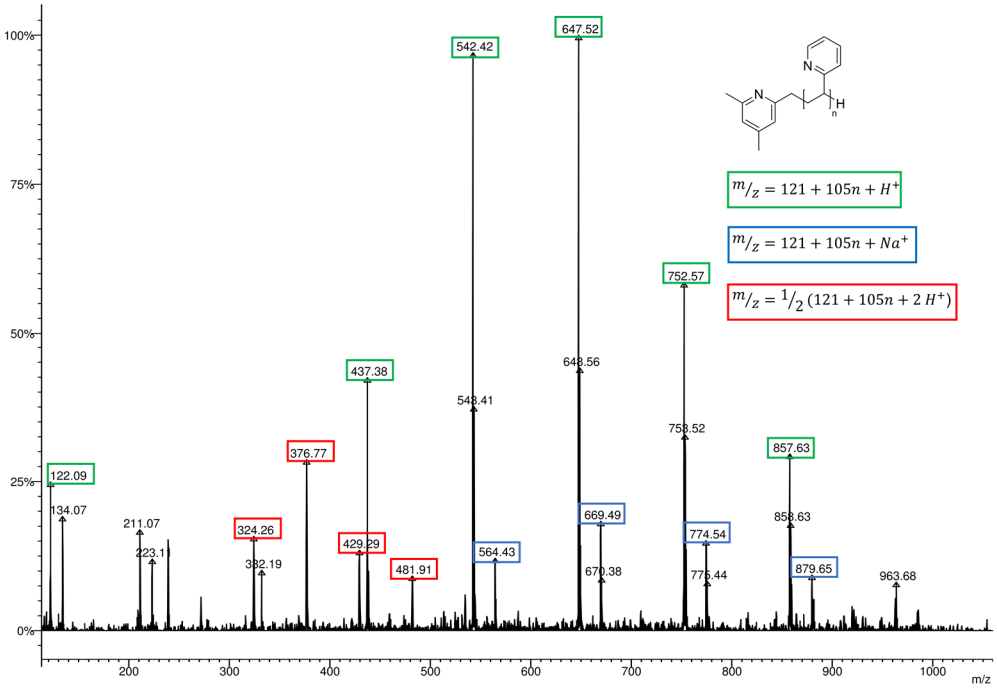

Fig. S6 ESI-MS spectrum of 2VP oligomers generated with complex **4** and *sym*-collidine as initiator.

4 Kinetic Investigation with Activated $Cp_2Y(CH_2TMS)(THF)$

Kinetic investigation with 2,3,5,6-Tetramethylpyrazine as initiator

102 mg $Cp_2Y(CH_2TMS)(THF)$ (**4**) (270 µmol, 2.00 equiv.) were dissolved in absolute toluene (4.00 mL) and treated with a solution of 2,3,5,6-tetramethylpyrazine (**1**) (135 µmol, 1.00 equiv.) in 2.00 mL absolute toluene. An instant orange colouration of the solution occurred, which indicated the successful C-H bond activation. After 16 hours ^{1}H-NMR spectroscopy confirmed the quantitative C-H bond activation. The solution was diluted with additional toluene (14.0 mL) and the polymerisation was started by addition of 2-vinylpyridine (2.84 g, 27.0 mmol, 200 equiv.) in one portion. Aliquots (circa 400 mg per sample) were taken in regular time intervals and poured into methanol (500 µL each). The aliquots were dried and then analysed by ^{1}H-NMR and GPC. After the complete conversion of 2-vinylpyridine, the reaction was terminated by addition of methanol (1.00 mL).

Kinetic investigation with *sym*-collidine as initiator

51.1 mg $Cp_2Y(CH_2TMS)(THF)$ (**4**) (135 µmol, 1.00 equiv.) were dissolved in absolute toluene (4.00 mL) and treated with a solution of *sym*-collidine (135 µmol, 1.00 equiv.) in 2.00 mL absolute toluene. An instant yellow colouration of the solution occurred, which indicated the successful C-H bond activation. After 16 hours ^{1}H-NMR spectroscopy confirmed the quantitative C-H bond activation. The solution was diluted with additional toluene (14.0 mL) and the polymerisation was started by addition of 2-vinylpyridine (2.84 g, 27.0 mmol, 200 equiv.) in one portion. Aliquots (circa 400 mg per sample) were taken in regular time intervals and poured into methanol (500 µL each). The aliquots were dried and then analysed by ^{1}H-NMR and GPC. After the complete conversion of 2-vinylpyridine, the reaction was terminated by addition of methanol (1.00 mL).

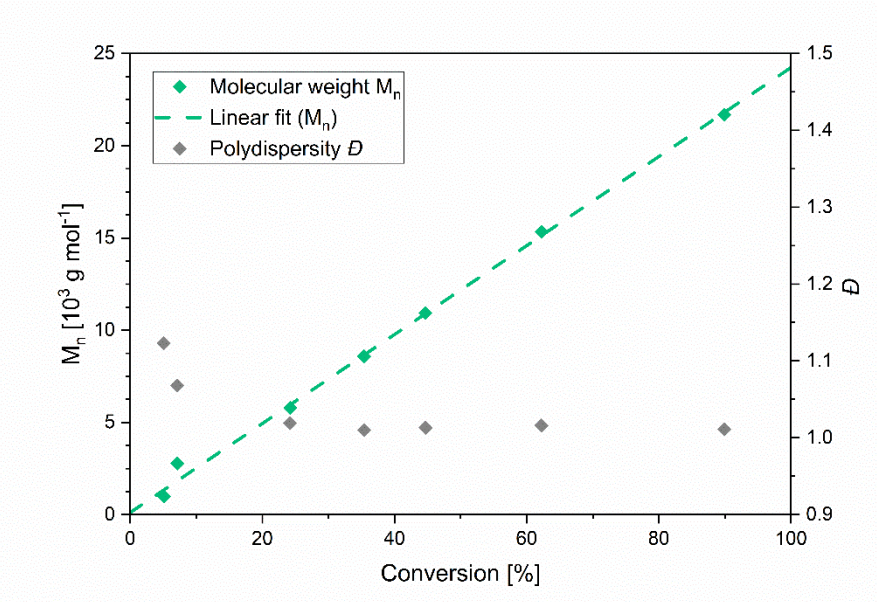

Fig. S7 Conversion-dependant plot of the molecular weights M_n and respective polydispersities $Đ$ of the P2VP aliquots generated with complex **4** and *sym*-collidine as initiator.

5 Synthesis and Characterisation of the Copolymers

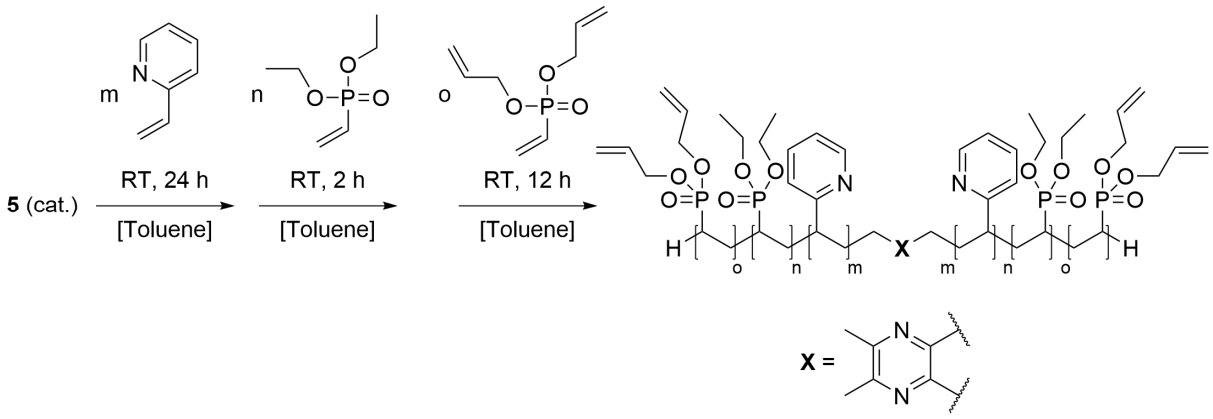

A solution of 2,3,5,6-tetramethylpyrazine (**1**) (1.00 equiv.) in dry toluene (1.00 mL) was added to a solution of $Cp_2Y(CH_2TMS)(THF)$ (**4**) (2.00 equiv.) in absolute toluene (1.00 mL). After the quantitative conversion was detected by ^{1}H-NMR spectroscopy, the reaction mixture was diluted with 8.00 mL of toluene and the respective amount of 2-vinylpyridine was added in one portion. After stirring overnight one aliquot was taken (0.1 mL quenched with 0.4 mL of MeOD-*d*$_4$), the conversion of 2-vinylpyridine was determined by ^{1}H-NMR and the calculated amount of DEVP was added to the solution in one portion. After two hours another aliquot was taken (0.1 mL quenched with 0.4 mL of MeOD-*d*$_4$) and the conversion of DEVP was determined *via* ^{31}P-NMR. For DAlVP the DEVP procedure was repeated. After ^{31}P-NMR had confirmed the full conversion of DAlVP, the reaction was quenched by addition of methanol (0.5 mL). After precipitation in pentane (200 mL) the clear solution was decanted off, volatiles were removed by drying at ambient temperature and the crude polymer was dissolved in water and freeze-dried.

Molecular weights M_n and the molecular weight distributions of the P2VP block were measured *via* GPC analysis of the first aliquot. The composition B'BABB' of the dried copolymer was determined *via* ^{1}H NMR spectroscopy. Molecular weights of the block copolymer were calculated on basis of the M_n of the P2VP block and the respective composition. The molecular weight distribution of the second sequence was also examined by GPC analysis.

Characterisation of BAB1 (100/200/10)

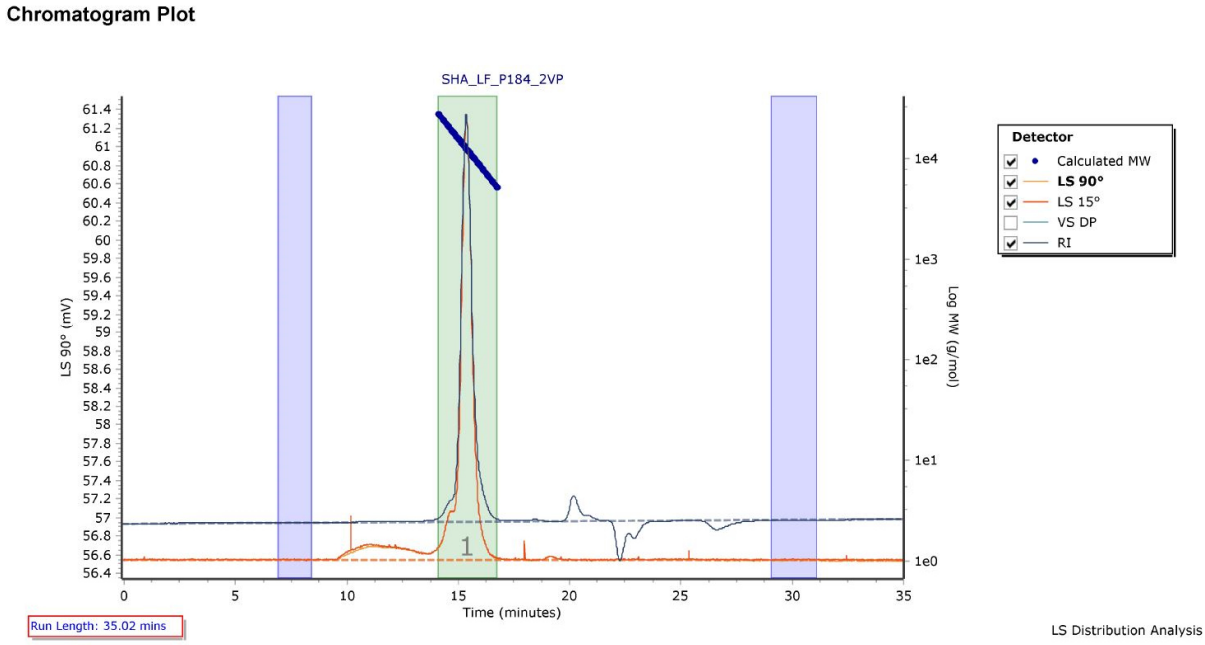

Fig. S8 GPC trace of P2VP block of **BAB1**.

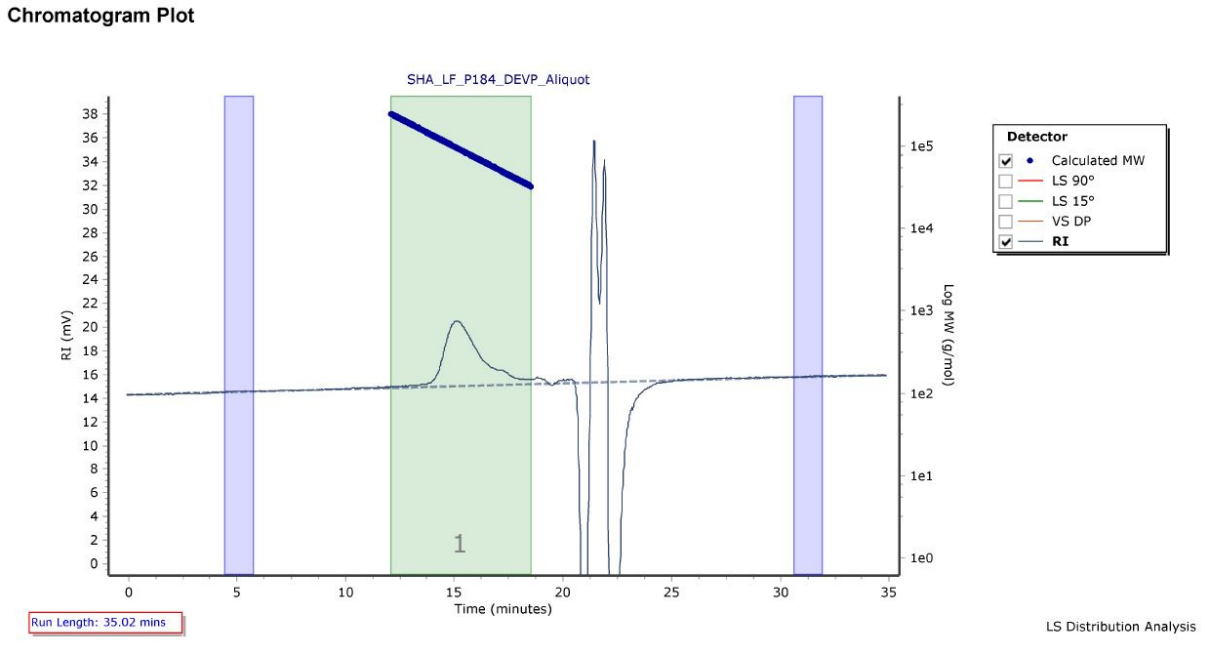

Fig. S9 GPC trace of P2VP-PDEVP blocks of **BAB1**.

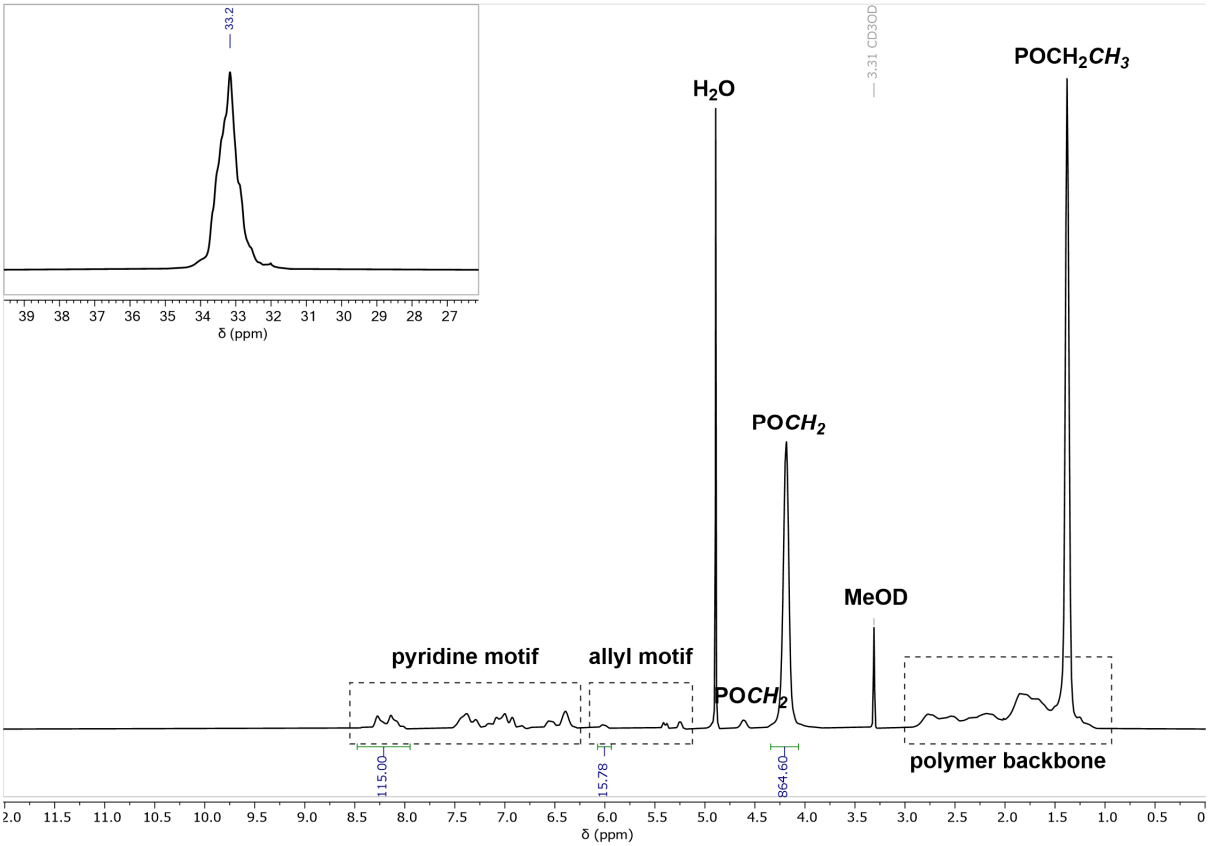

Fig. S10 ^{1}H-NMR and ^{31}P-NMR of **BAB1** in MeOD-*d*$_4$.

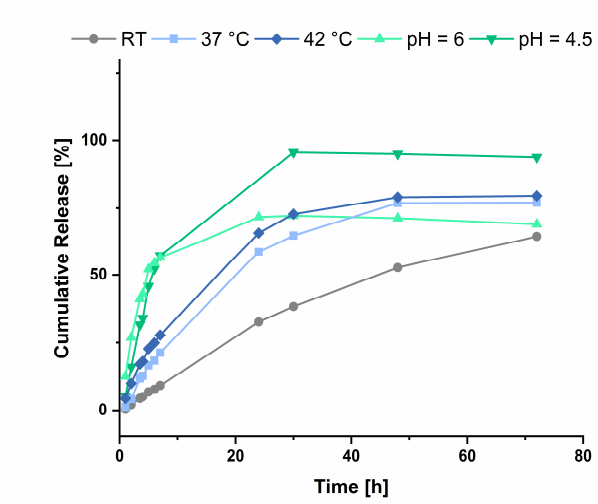

Fig. S11 Cumulative release of fluorescein from **BAB1** under varying conditions.

Characterisation of BAB2 (200/200/10)

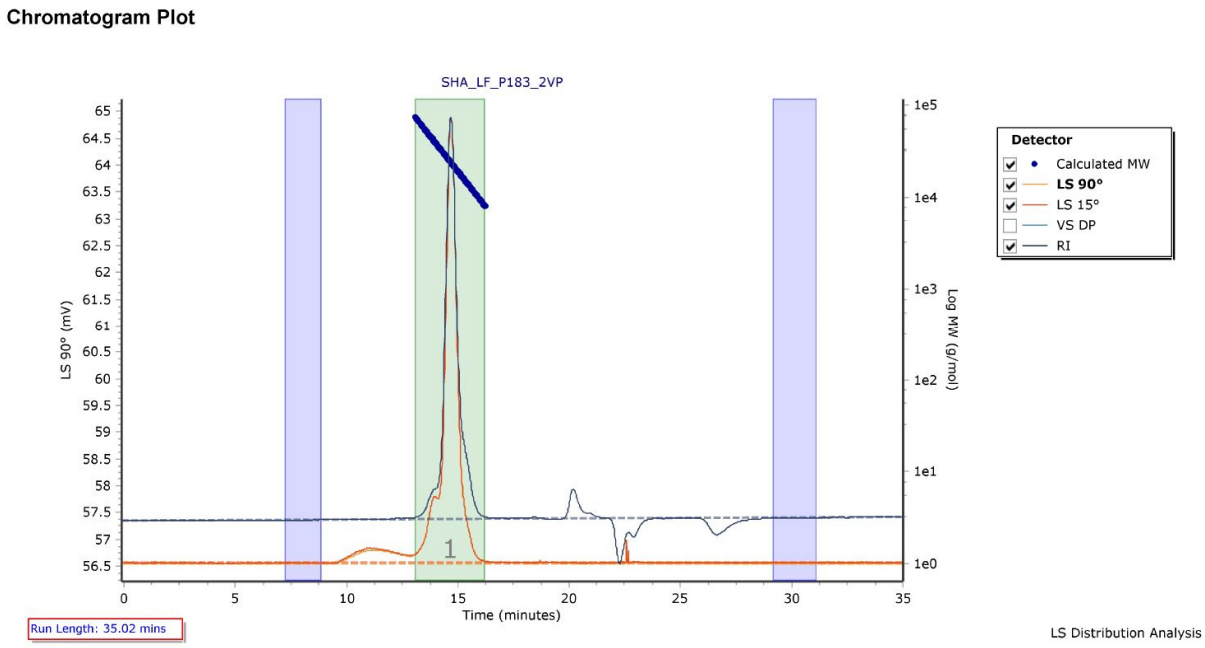

Fig. S12 GPC trace of P2VP block of **BAB2**.

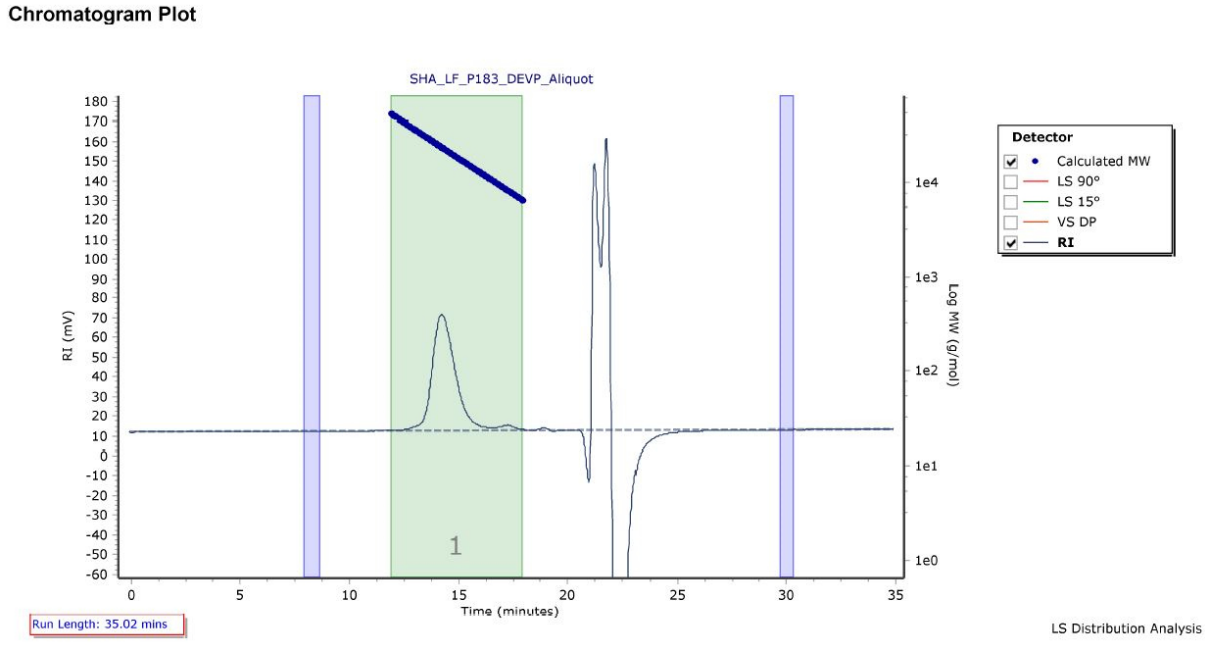

Fig. S13 GPC trace of P2VP-PDEVP blocks of **BAB2**.

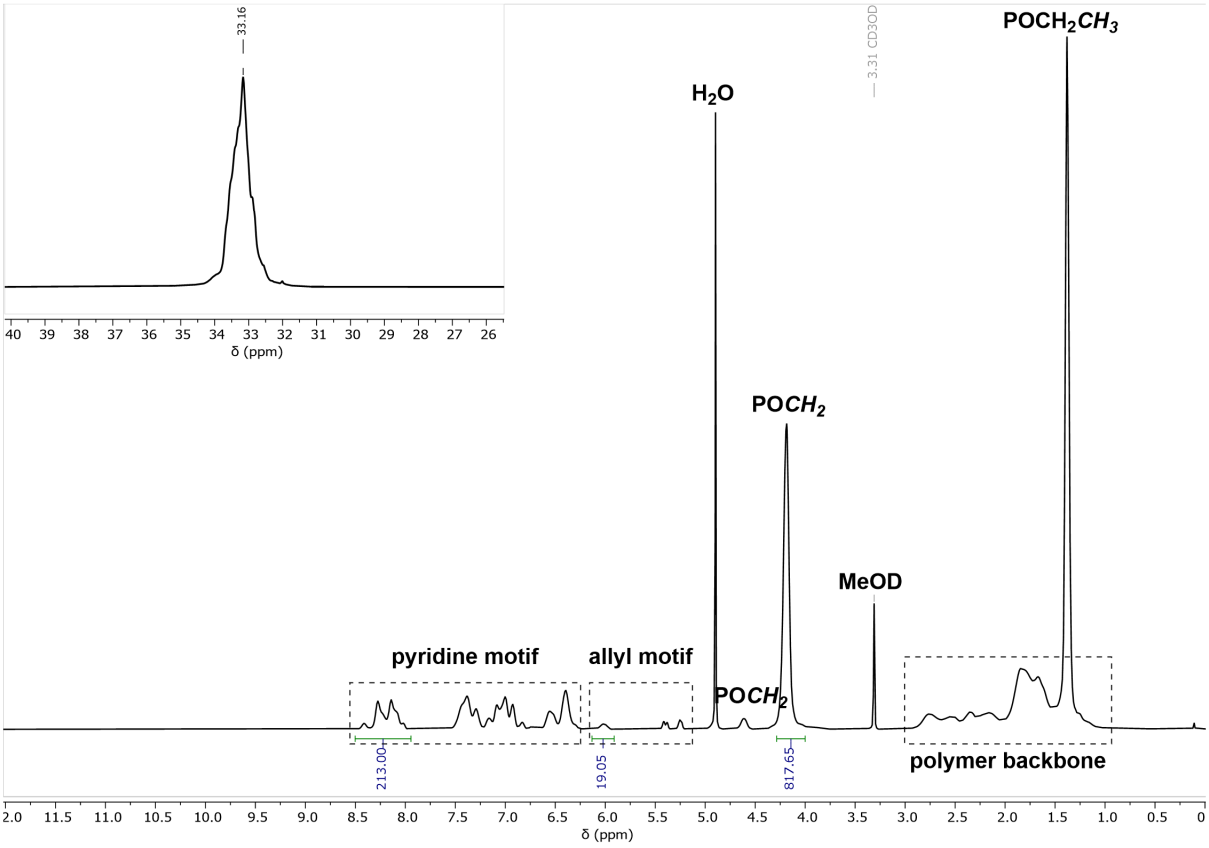

Fig. S14 ^{1}H-NMR and ^{31}P-NMR of **BAB2** in MeOD-d_4.

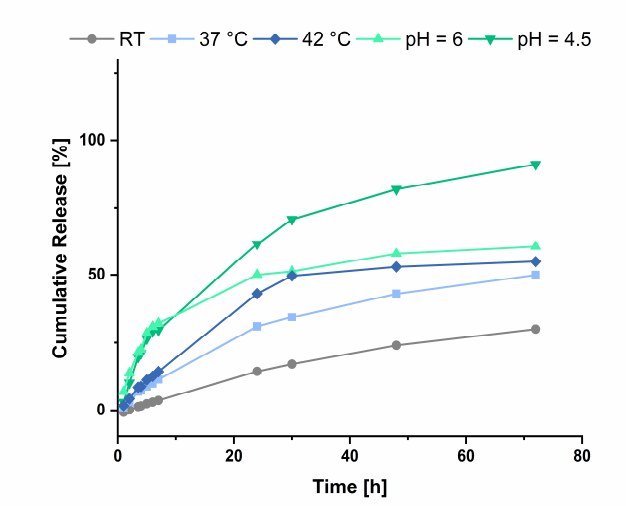

Fig. S15 Cumulative release of fluorescein from **BAB2** under varying conditions.

Characterisation of BAB3 (300/300/10)

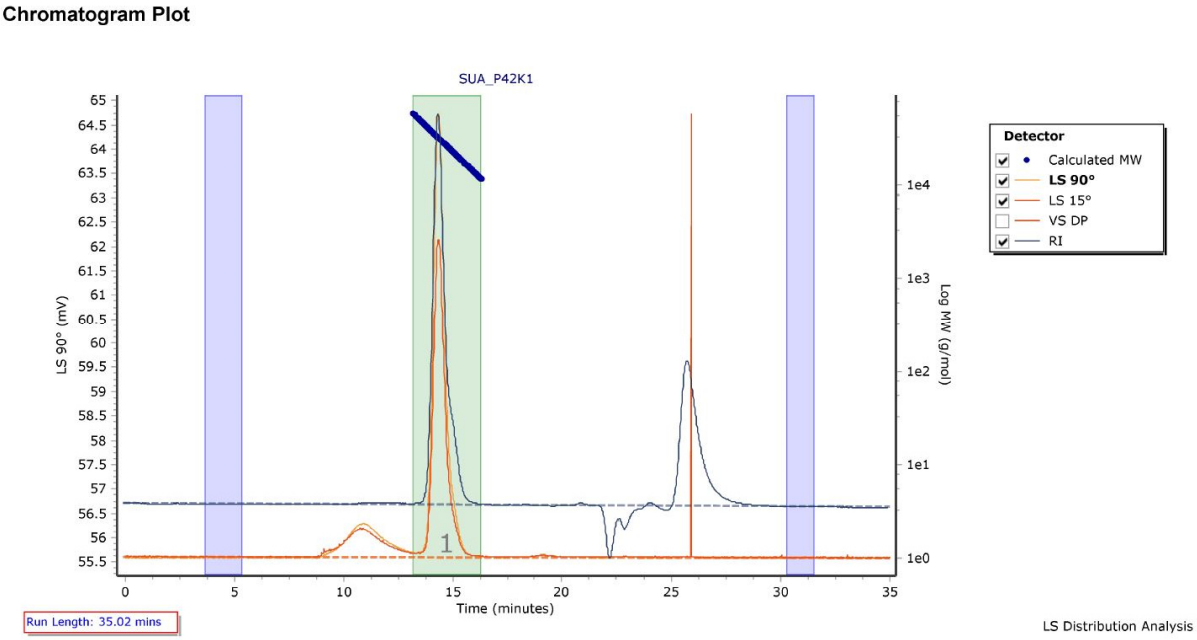

Fig. S16 GPC trace of P2VP block of **BAB3**.

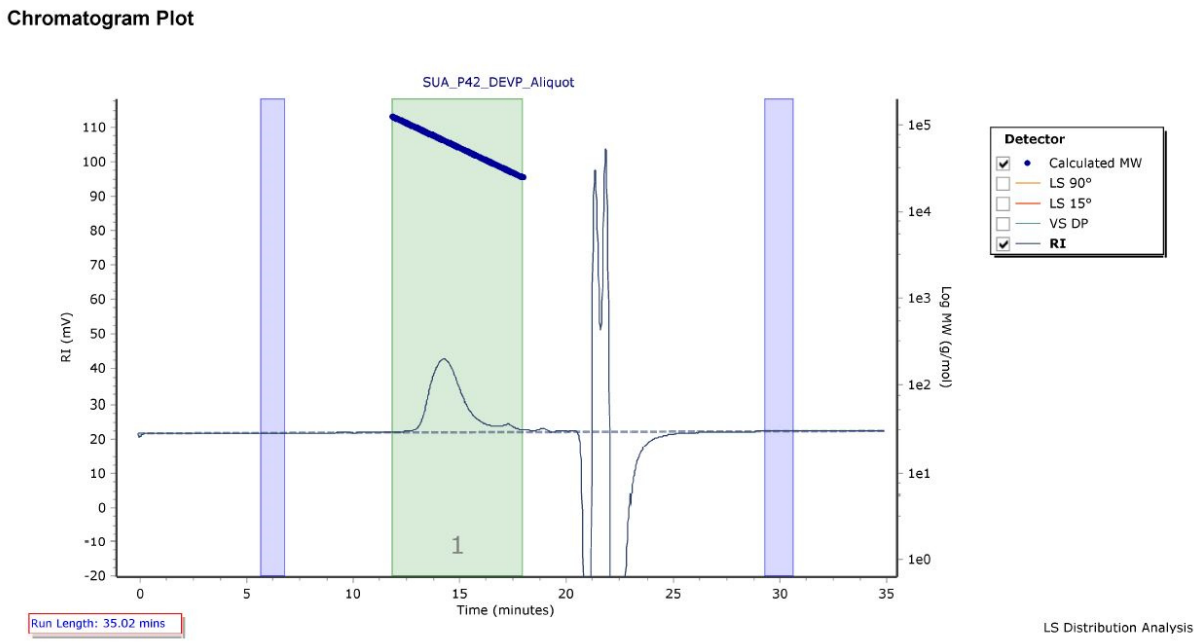

Fig. S17 GPC trace of P2VP-PDEVP blocks of **BAB3**.

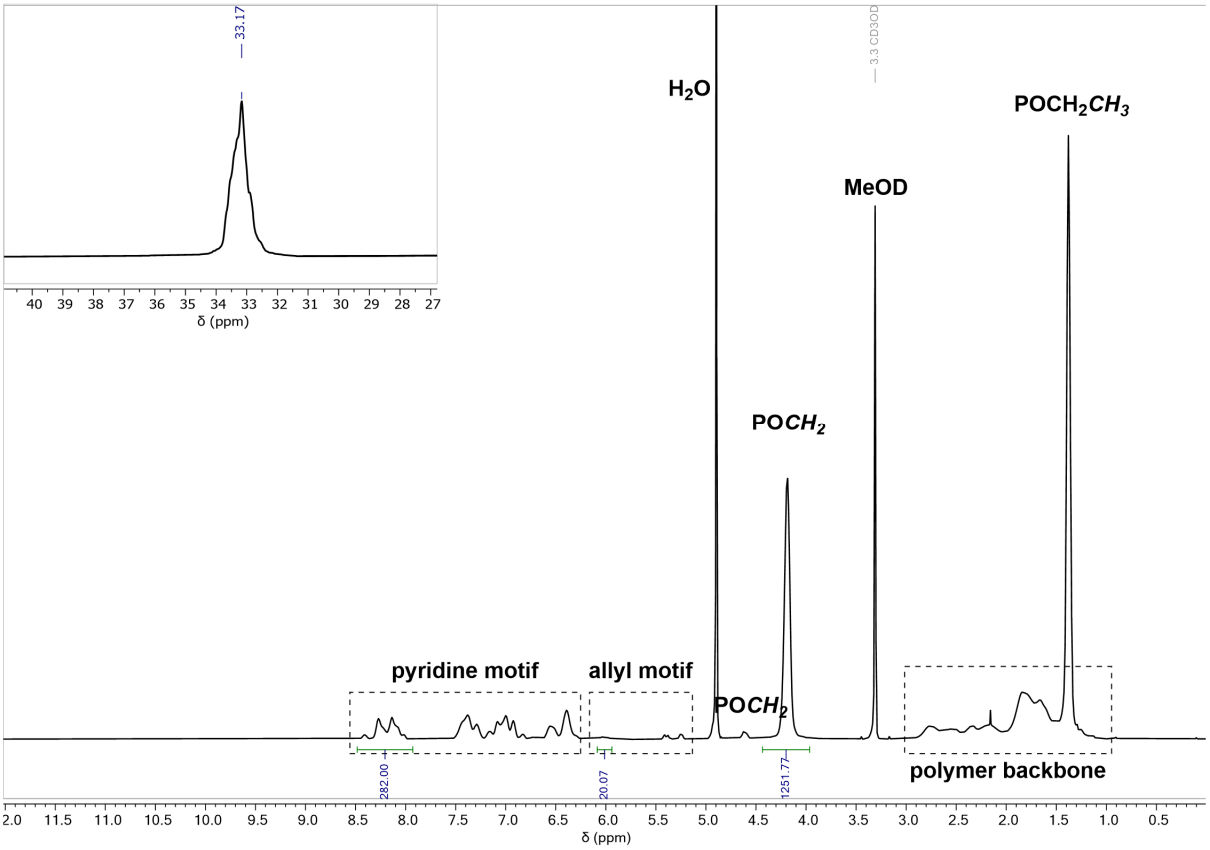

Fig. S18 ^{1}H-NMR and ^{31}P-NMR of **BAB3** in MeOD-d_4.

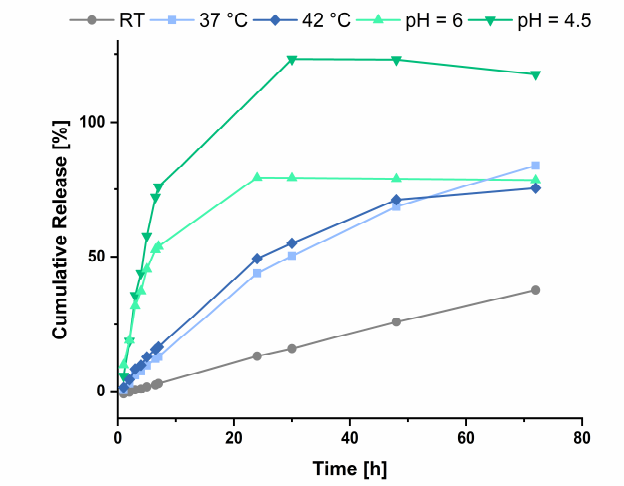

Fig. S19 Cumulative release of fluorescein from **BAB3** under varying conditions.

Characterisation of BAB4 (200/200/6)

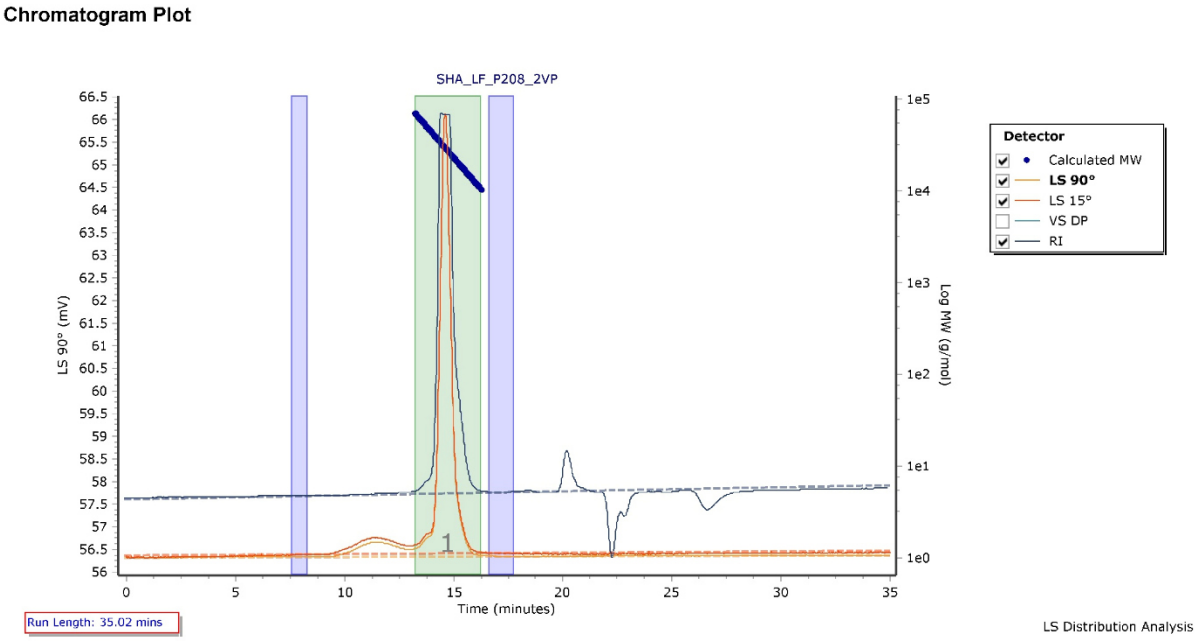

Fig. S20 GPC trace of P2VP blocks of **BAB4**.

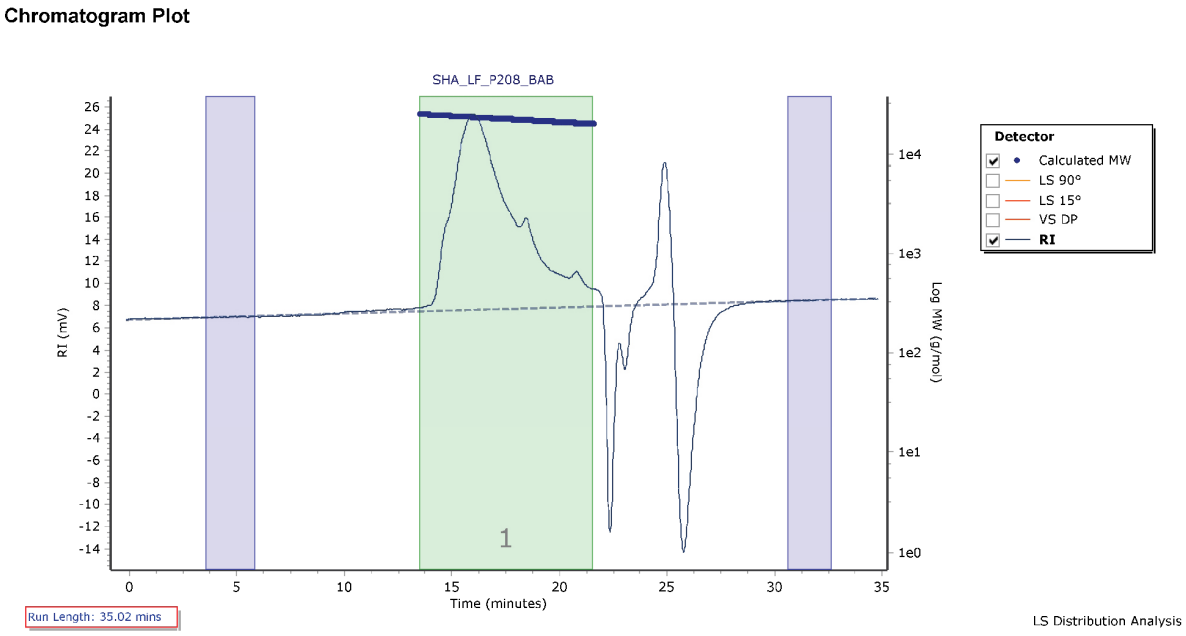

Fig. S21 GPC trace of P2VP-PDEVP blocks of **BAB4**.

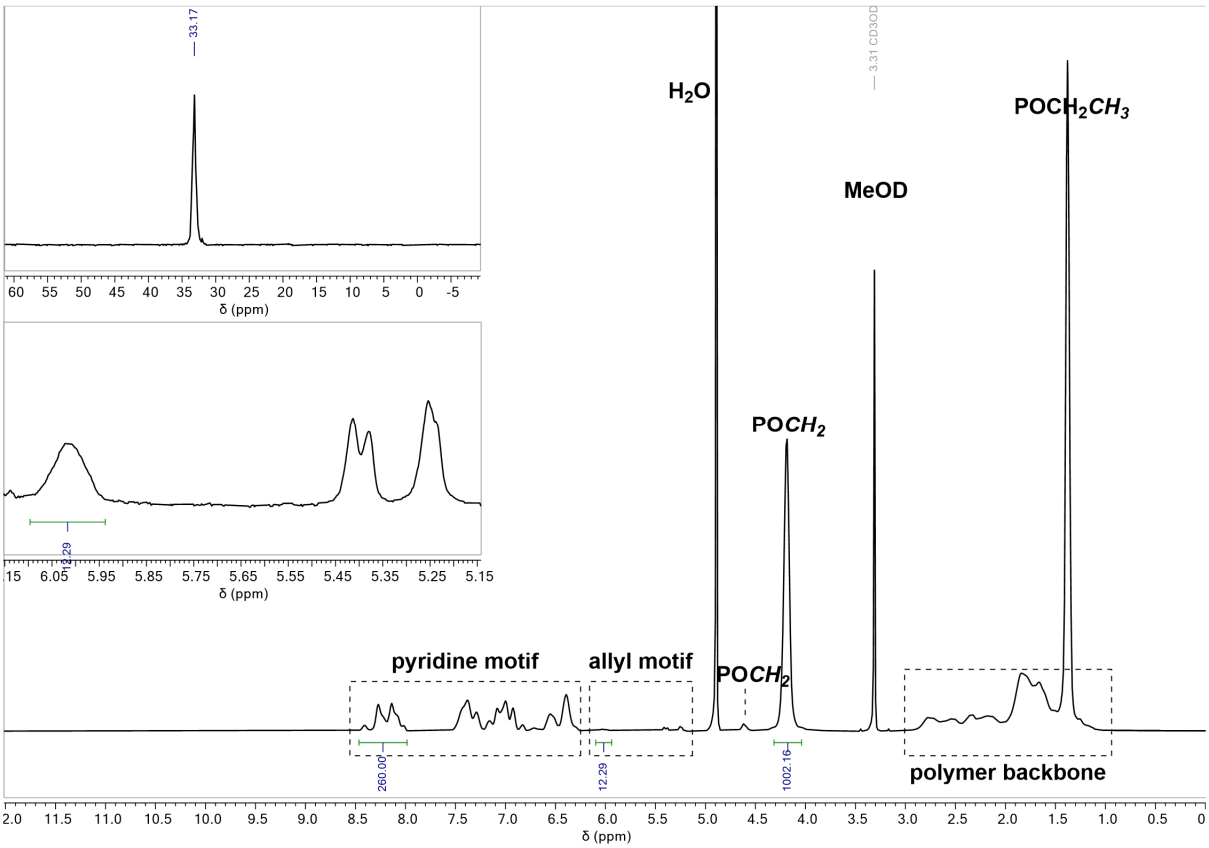

Fig. S22 ^{1}H-NMR and ^{31}P-NMR of **BAB4** in MeOD-*d*$_4$. Zoomed-in view of allylic protons.

Characterisation of BAB5 (200/200/20)

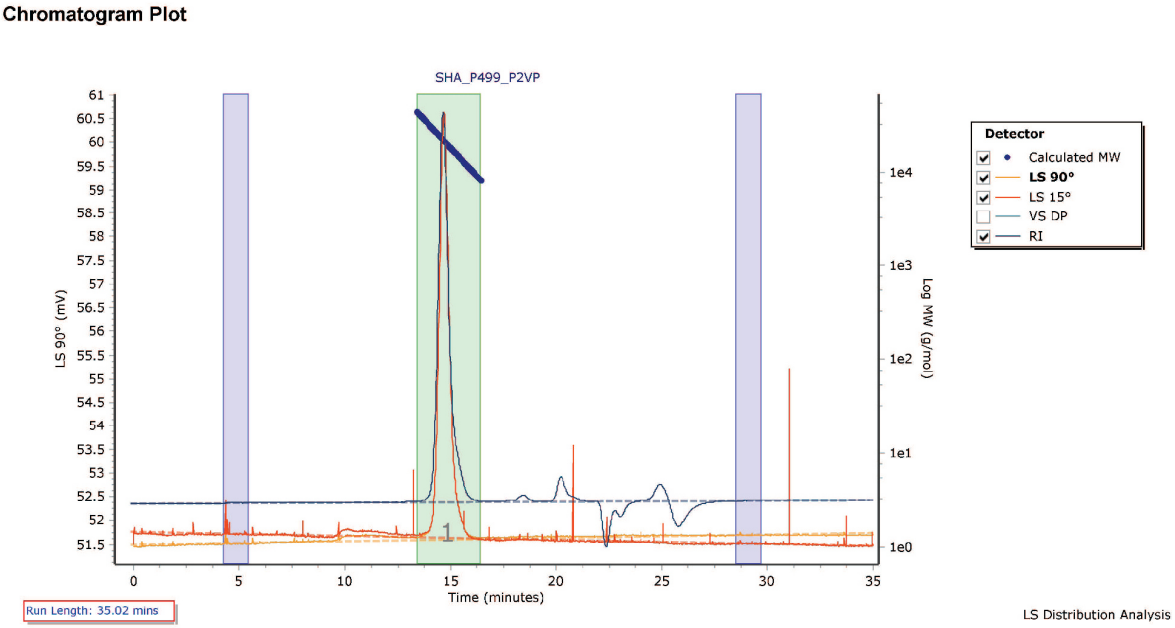

Fig. S23 GPC trace of P2VP block of **BAB5**.

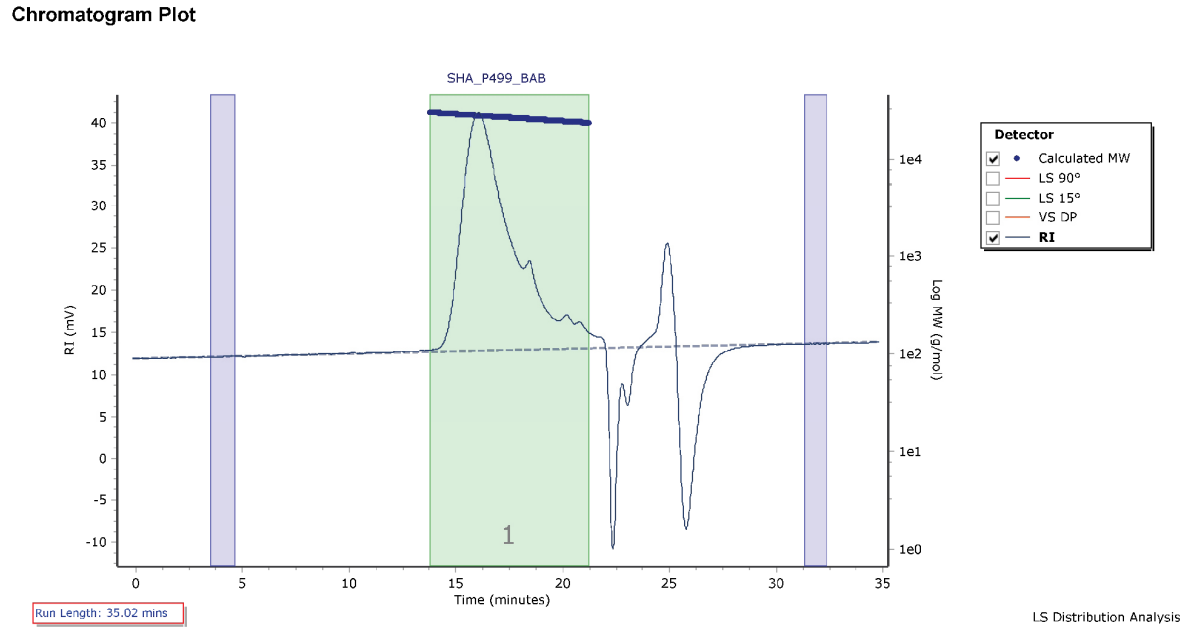

Fig. S24 GPC trace of P2VP-PDEVP block of **BAB5**.

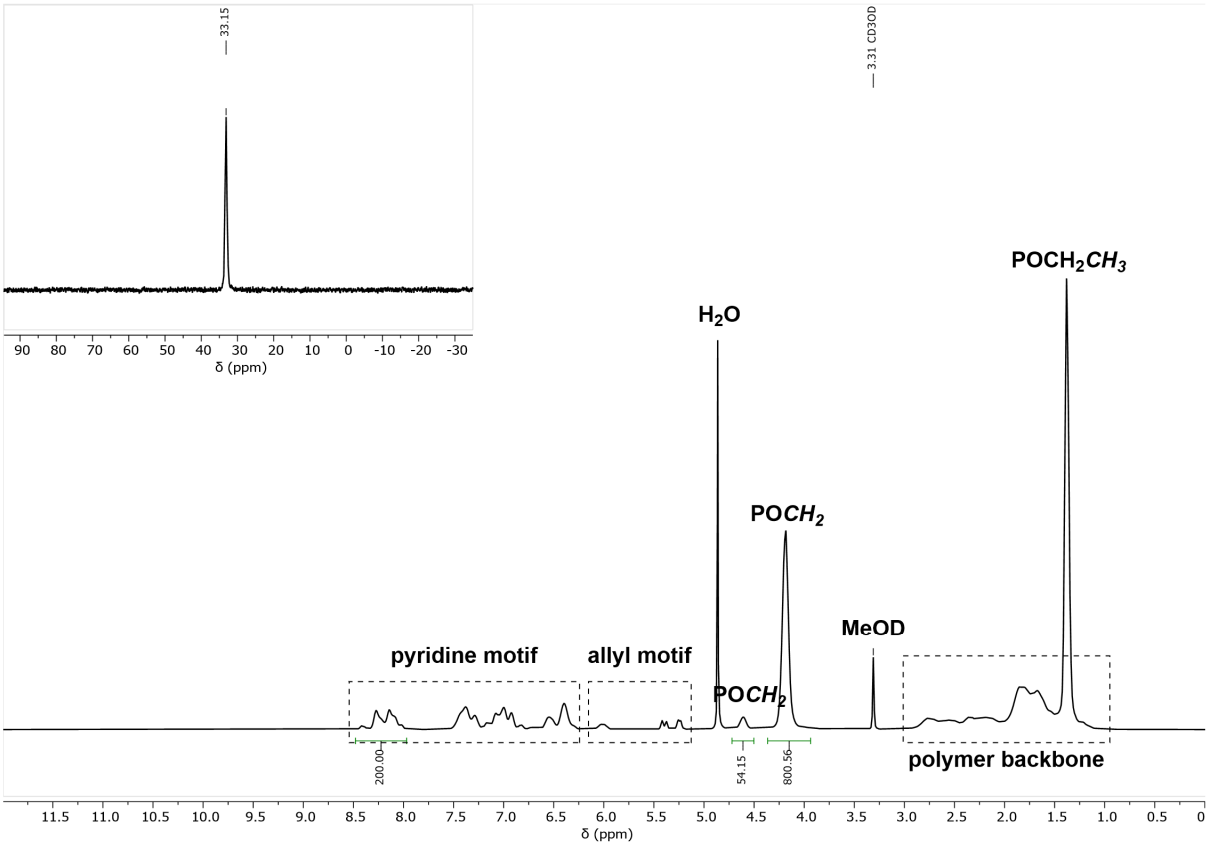

Fig. S25 ^{1}H-NMR and ^{31}P-NMR of **BAB5** in MeOD-d_4.

General procedure for the cross-linking with dithiols 6,7, and 8

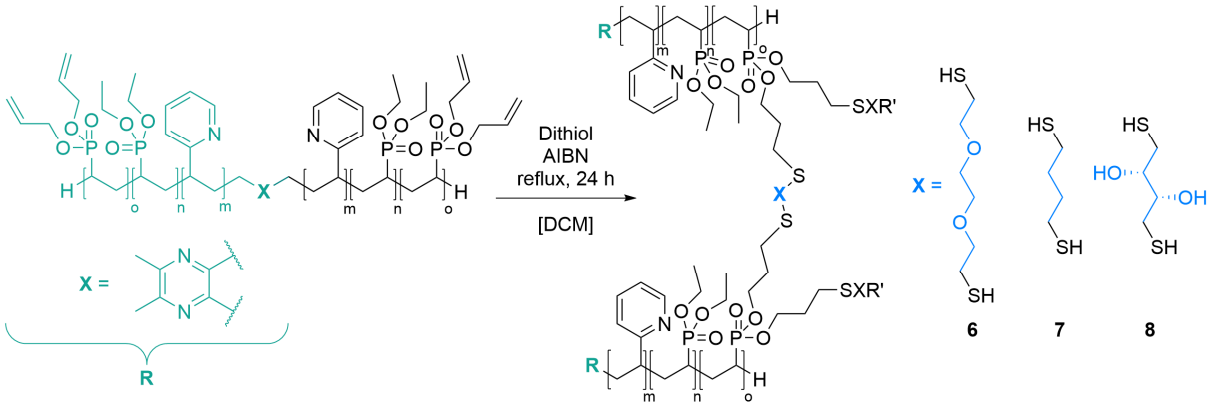

The corresponding copolymer was dissolved in methylene chloride (100 mg per 10 mL DCM) and treated with the respective dithiol (1.50 equiv. of dithiol per allyl group). It is recommended to prepare standard solutions of the dithiols. After addition of catalytic amounts of AIBN, the solution was degassed by the repeated evacuation of the reaction volume and filling with argon (20 iterations). The mixture was refluxed for 24 hours and the reaction progress was checked by proton NMR. After complete conversion of the allyl groups, volatiles were removed in vacuo, and the residue was dissolved in deionised water and purified by dialyses against water. Freeze-drying from water yielded the colourless product.

Characterisation of NP1 (100/200/10 - 3 6-dioxa-1,8-octanedithiol (6))

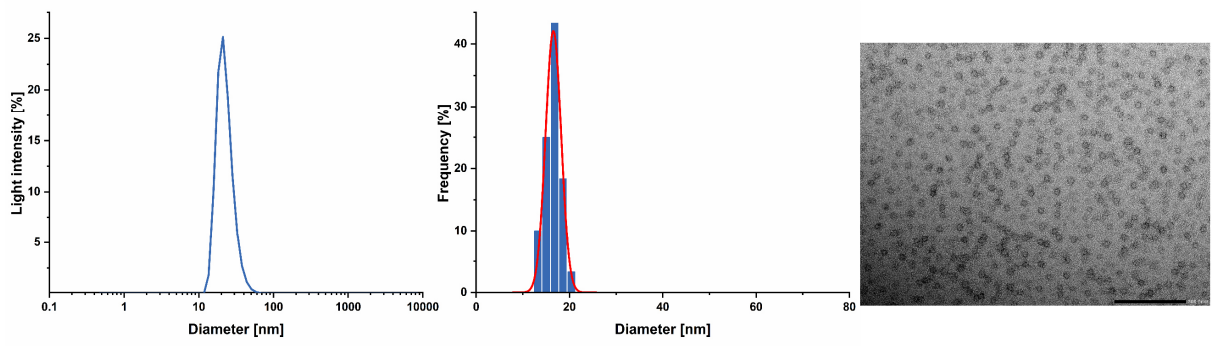

Fig. S26 Size distribution of **NP1** determined *via* DLS measurements at a concentration of 2.5 mg mL^{-1} in *Millipore* water (left); histogram plot with a gaussian regression fit (middle); and a TEM image of **NP1** (right) with a scale bar of 200 nm.

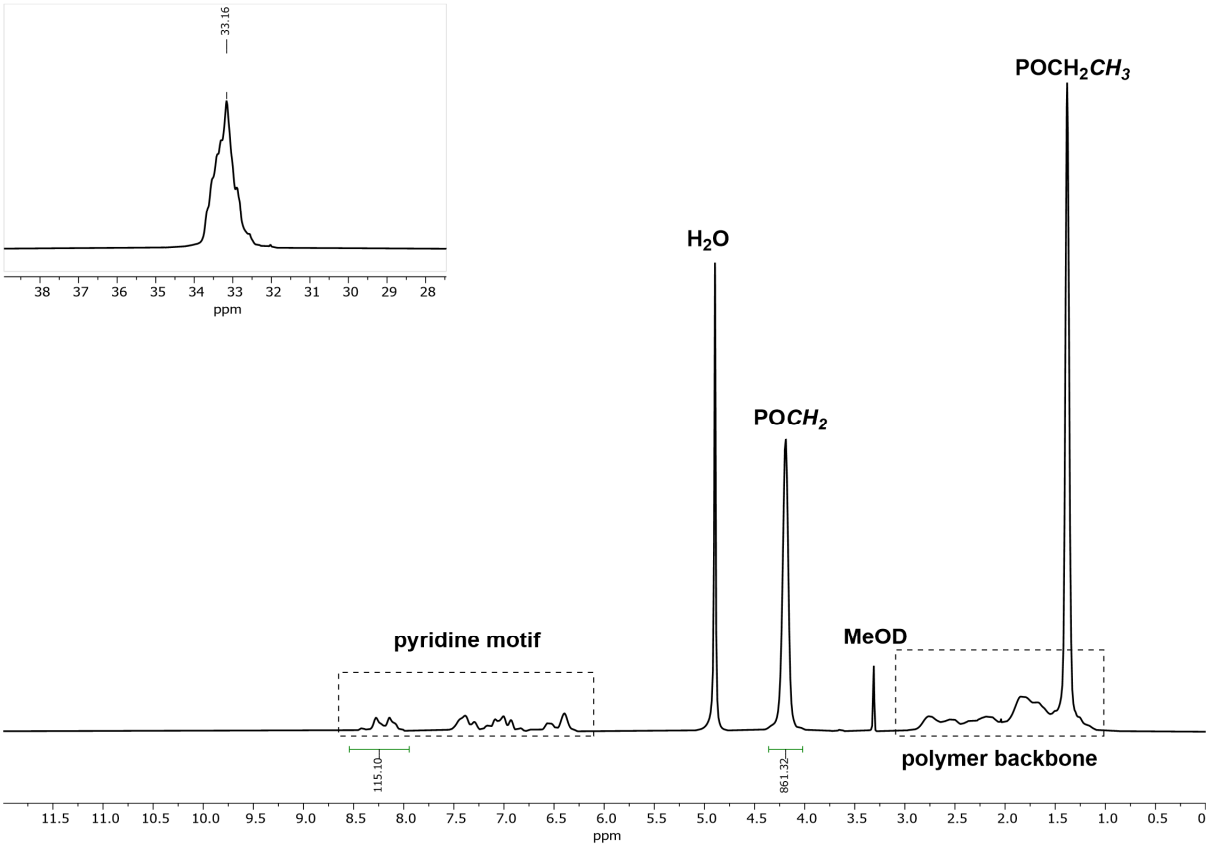

Fig. S27 ^{1}H-NMR and ^{31}P-NMR of **NP1** in MeOD-*d*$_4$.

Characterisation of NP2 (200/200/10 - 3 6-dioxa-1,8-octanedithiol (6))

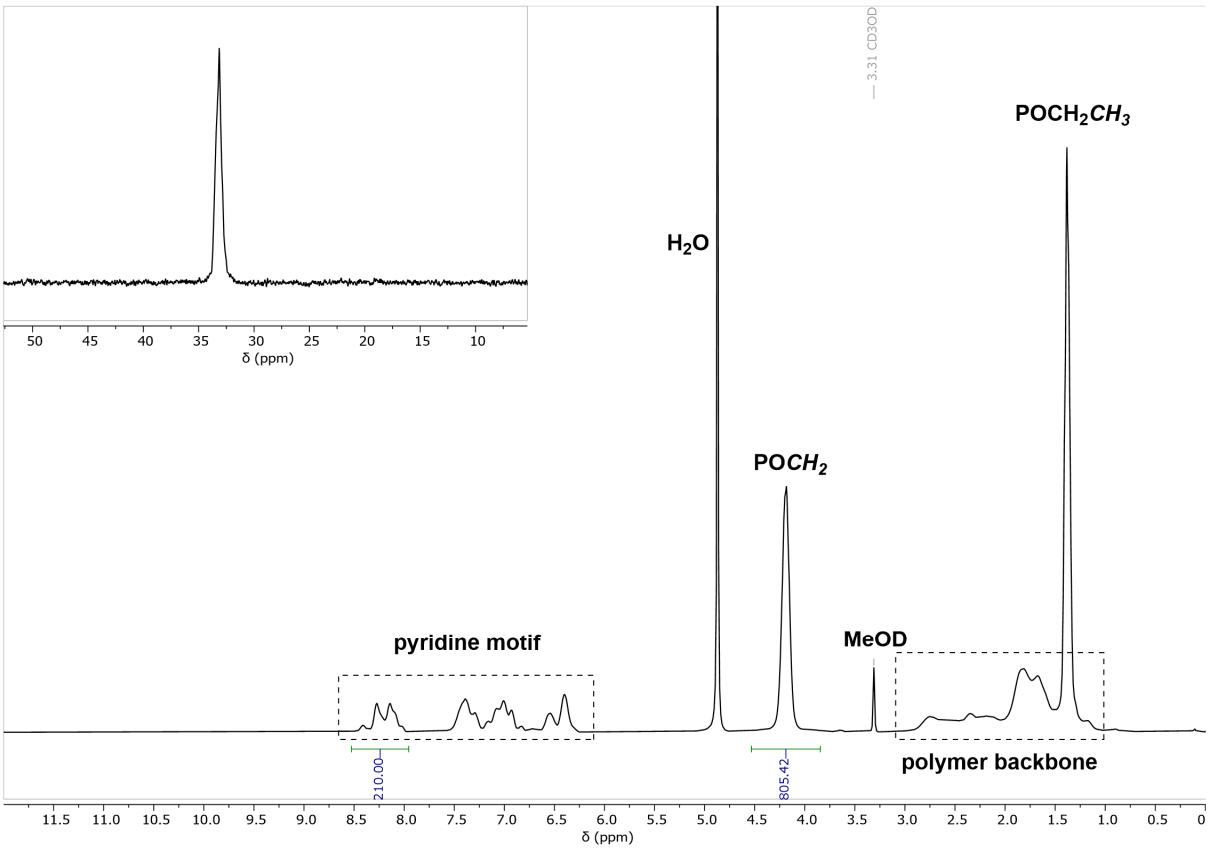

Fig. S28 ^{1}H-NMR and ^{31}P-NMR of **NP2** in MeOD-*d*$_4$.

Characterisation of NP3 (300/300/10 - 3 6-dioxa-1,8-octanedithiol (6))

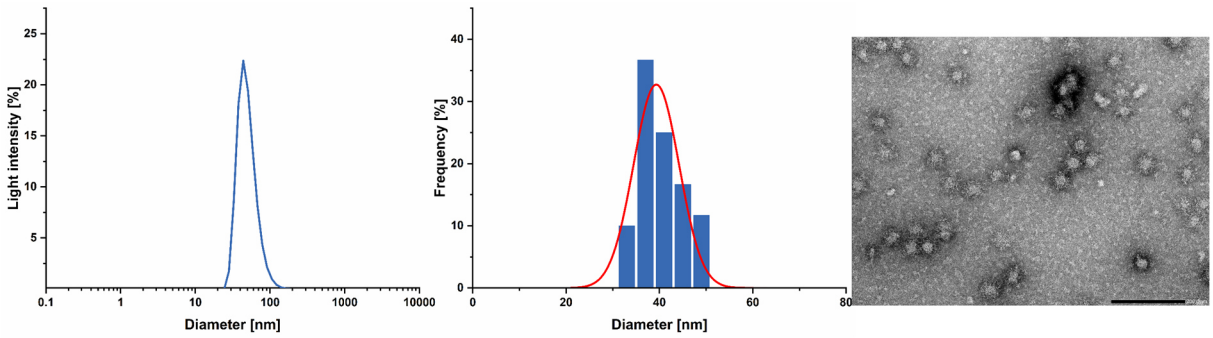

Fig. S29 Size distribution of **NP3** determined *via* DLS measurements at a concentration of 2.5 mg mL^{-1} in *Millipore* water (left); histogram plot with a gaussian regression fit (middle); and a TEM image of **NP3** (right) with a scale bar of 200 nm.

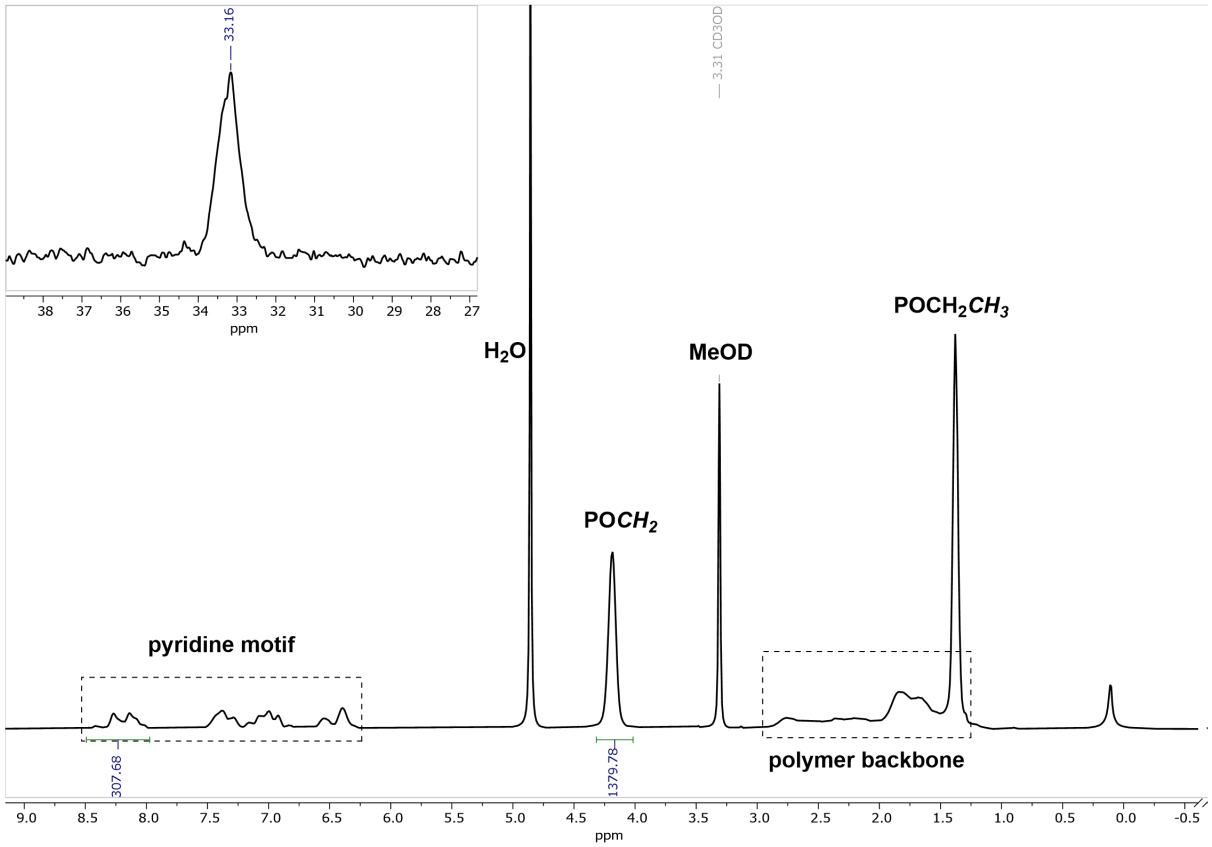

Fig. S30 ^{1}H-NMR and ^{31}P-NMR of **NP3** in MeOD-d_4.

Characterisation of NP4 (200/200/6 - 3 6-dioxa-1,8-octanedithiol (6))

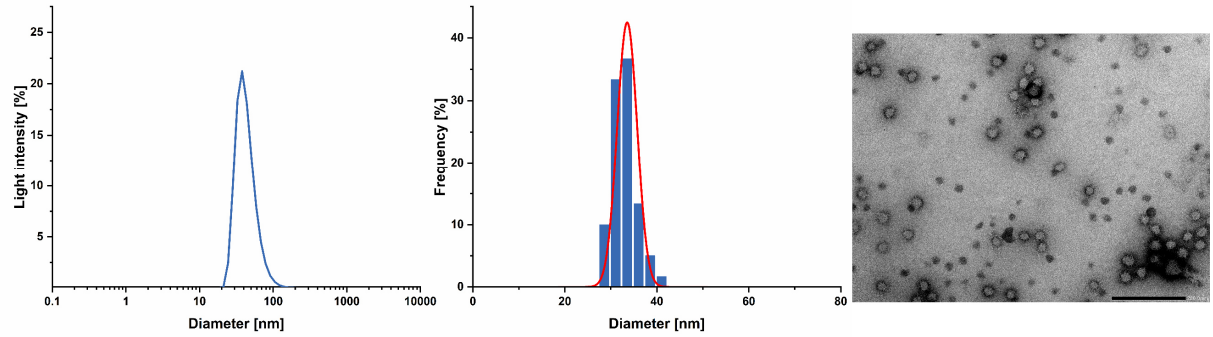

Fig. S31 Size distribution of **NP4** determined *via* DLS measurements at a concentration of 2.5 mg mL^{-1} in *Millipore* water (left); histogram plot with a gaussian regression fit (middle); and a TEM image of **NP4** (right) with a scale bar of 200 nm.

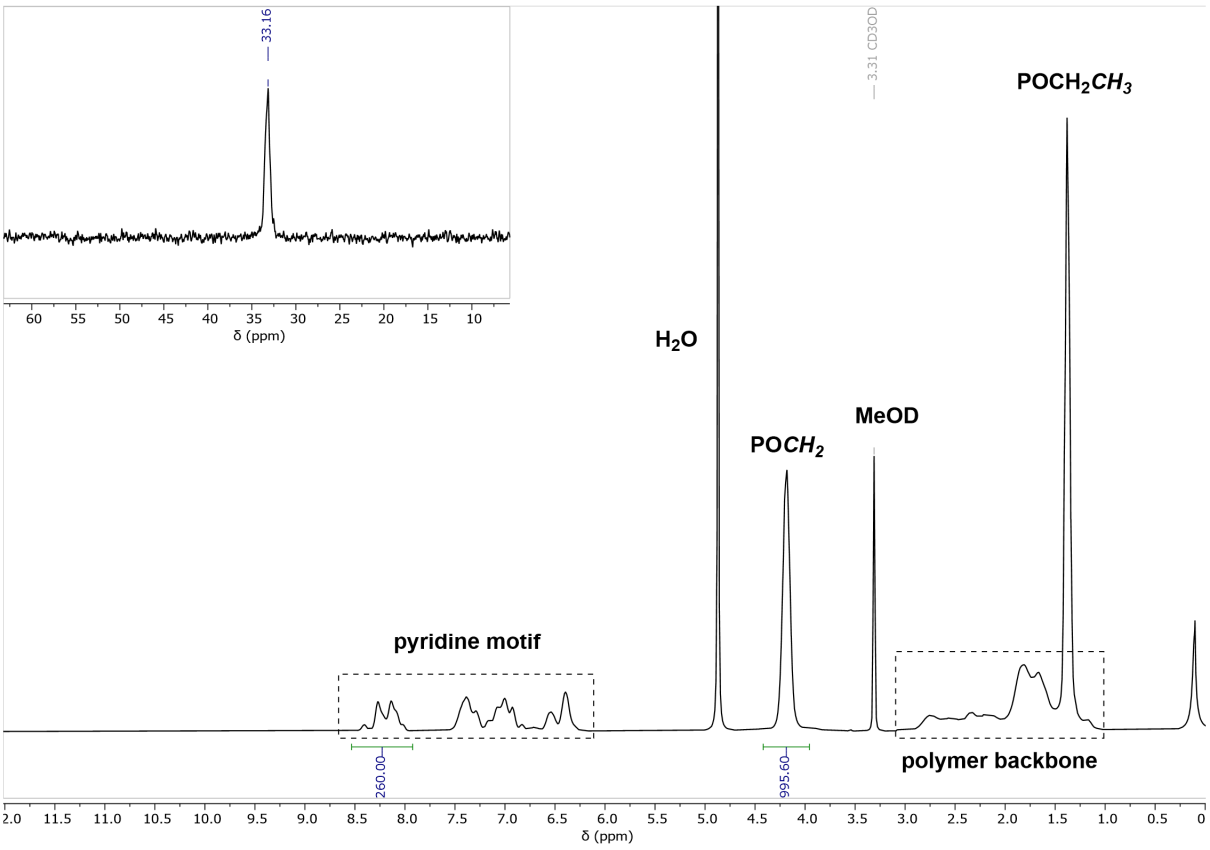

Fig. S32 ^{1}H-NMR and ^{31}P-NMR of **NP4** in MeOD-d_4.

Characterisation of NP5 (200/200/20 - 3 6-dioxa-1,8-octanedithiol (6))

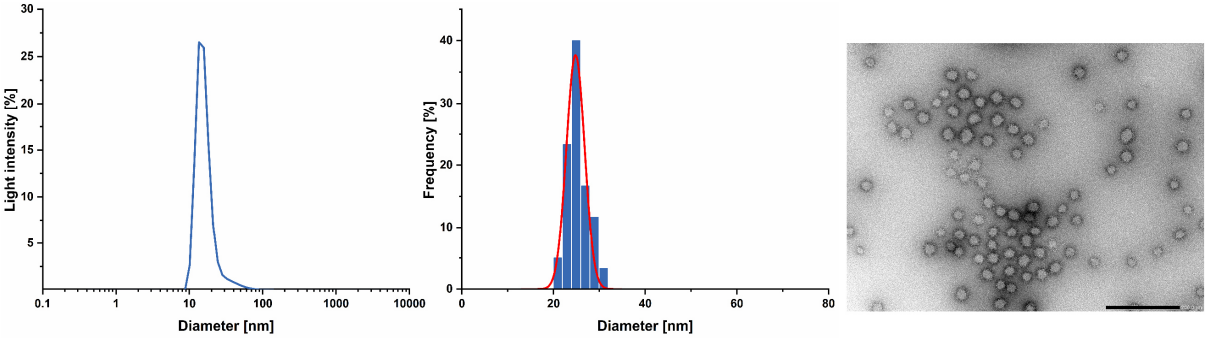

Fig. S33 Size distribution of **NP5** determined *via* DLS measurements at a concentration of 2.5 mg mL^{-1} in *Millipore* water (left); histogram plot with a gaussian regression fit (middle); and a TEM image of **NP5** (right) with a scale bar of 200 nm.

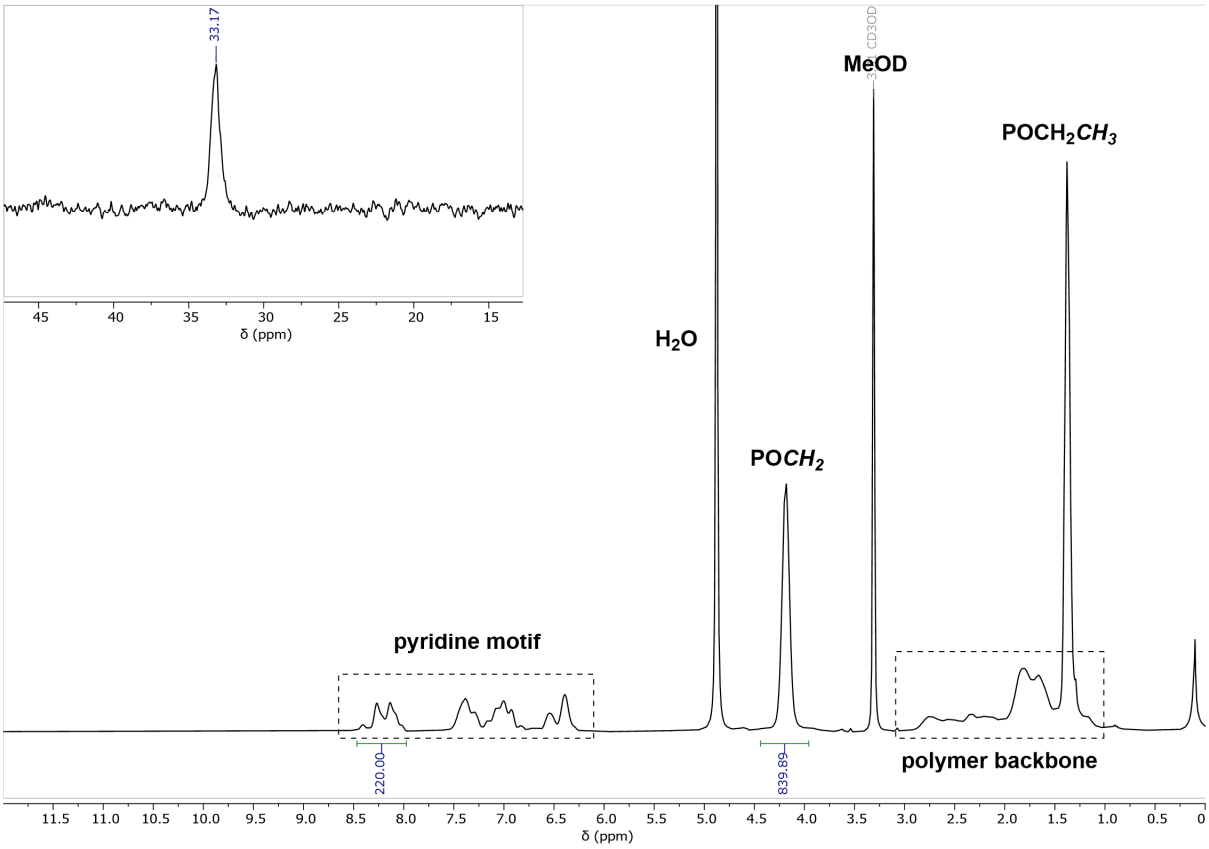

Fig. S34 ^{1}H-NMR and ^{31}P-NMR of **NP5** in MeOD-d_4.

Characterisation of NP6 (200/200/10 – 1,4-butanedithiol (7))

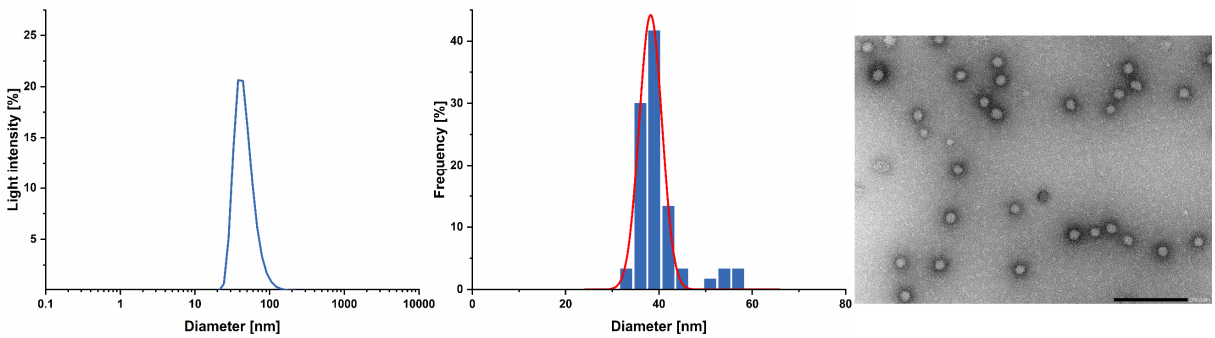

Fig. S35 Size distribution of **NP6** determined *via* DLS measurements at a concentration of 2.5 mg mL^{-1} in *Millipore* water (left); histogram plot with a gaussian regression fit (middle); and a TEM image of **NP6** (right) with a scale bar of 200 nm.

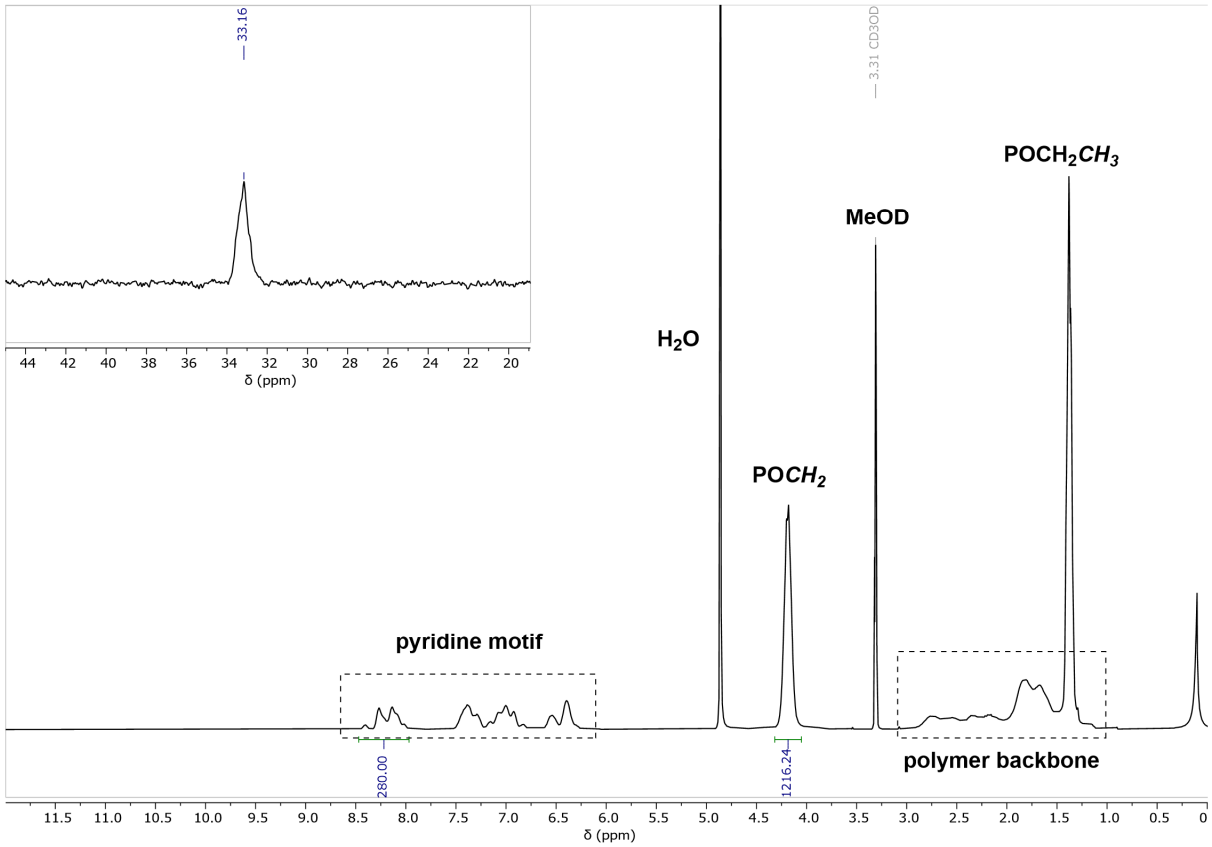

Fig. S36 ^{1}H-NMR and ^{31}P-NMR of **NP6** in MeOD-d_4.

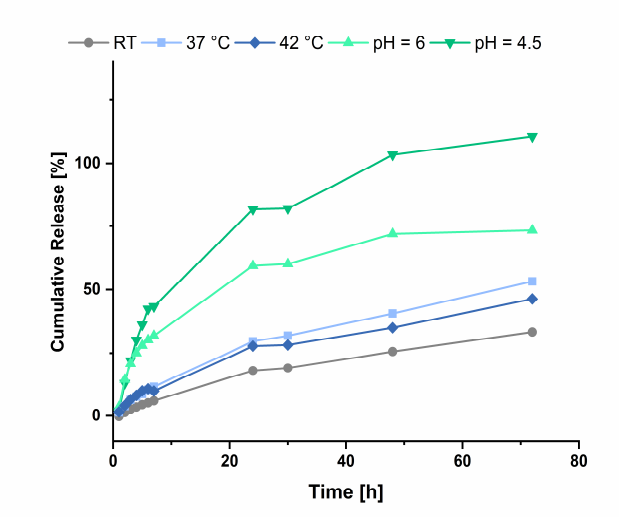

Fig. S37 Cumulative release of fluorescein from **NP6** under varying conditions.

Characterisation of NP7 (200/200/10 – D,L-dithiothreitol (8))

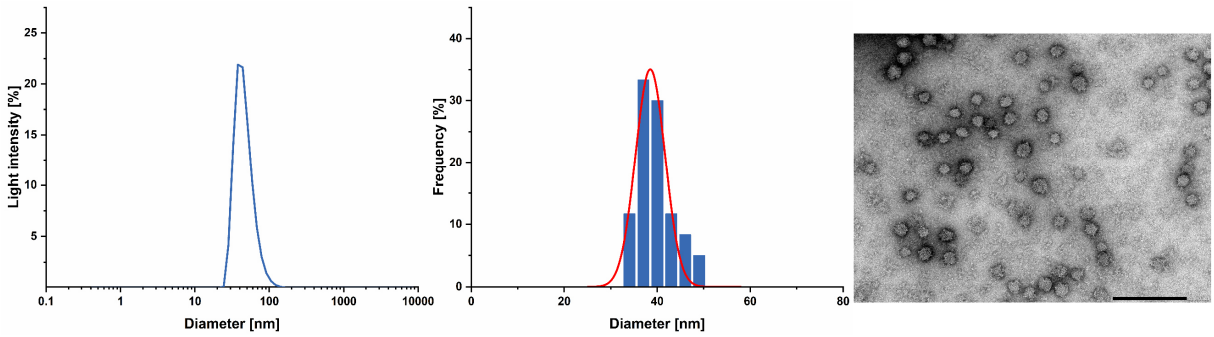

Fig. S38 Size distribution of **NP7** determined *via* DLS measurements at a concentration of 2.5 mg mL^{-1} in *Millipore* water (left); histogram plot with a gaussian regression fit (middle); and a TEM image of **NP7** (right) with a scale bar of 200 nm.

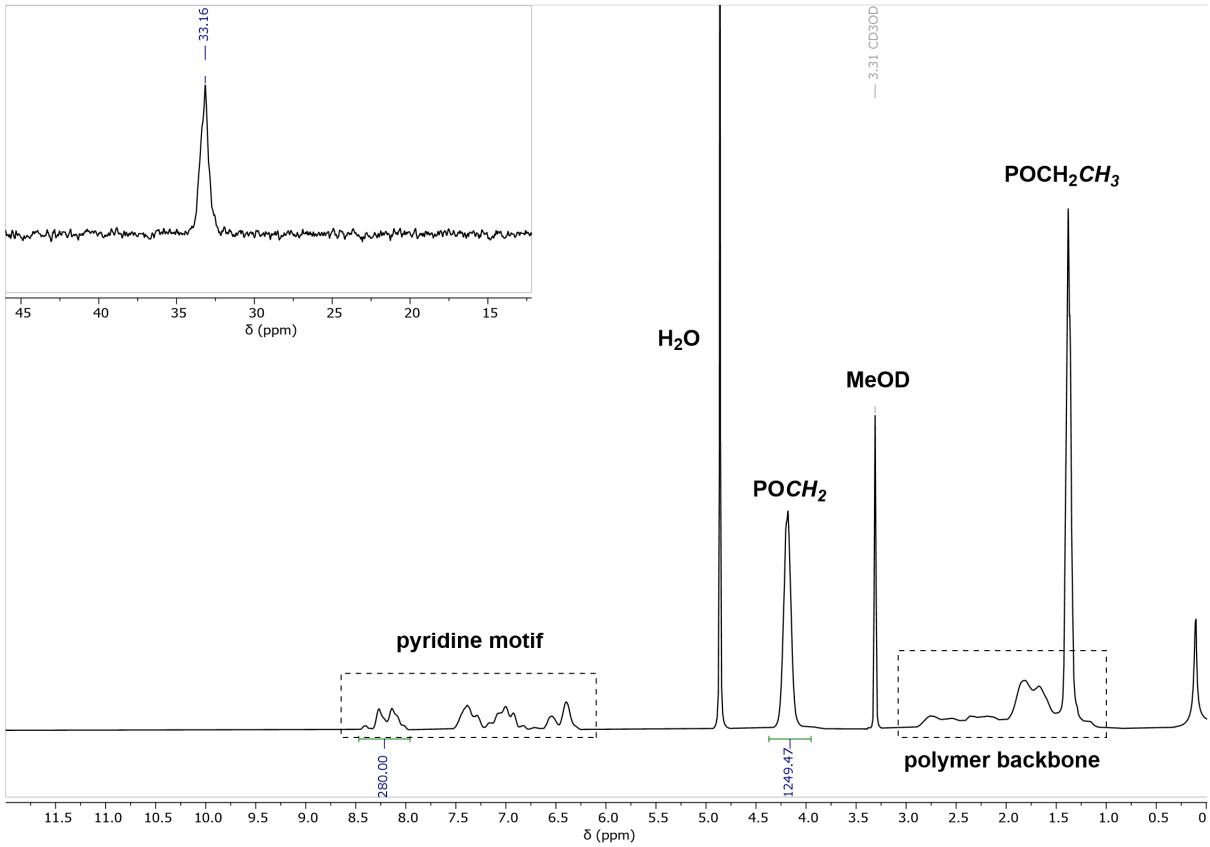

Fig. S39 ^{1}H-NMR and ^{31}P-NMR of **NP7** in MeOD-d_4.

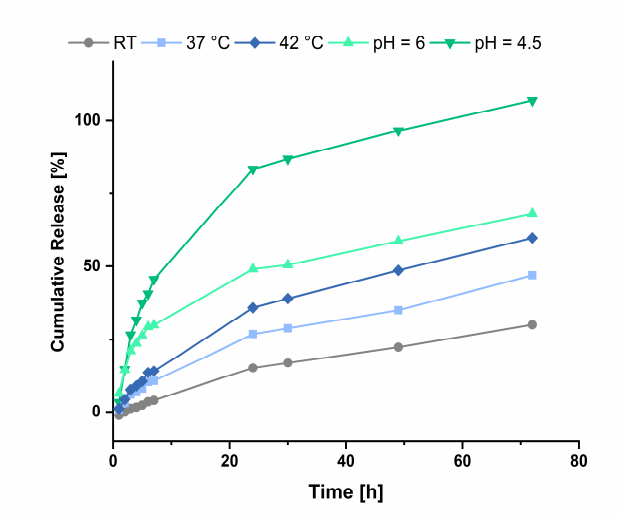

Fig. S40 Cumulative release of fluorescein from **NP7** under varying conditions.

Stability of NP1-NP7 in Chloroform

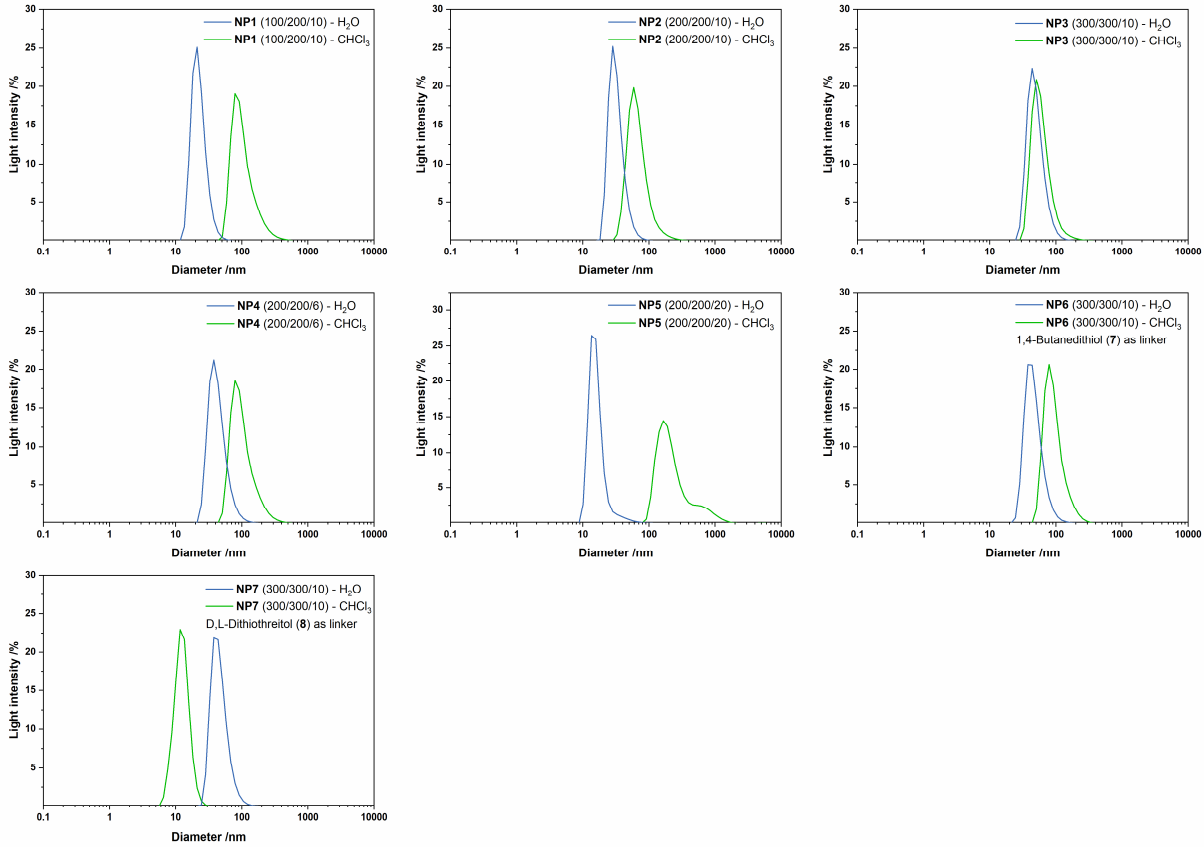

Fig. S41 Size distribution of **NP1-NP7** in *Millipore* water (blue) and chloroform (green) determined via DLS at a concentration of 2.5 mg mL^{-1}.

Determination of the LCST of NP1-NP7

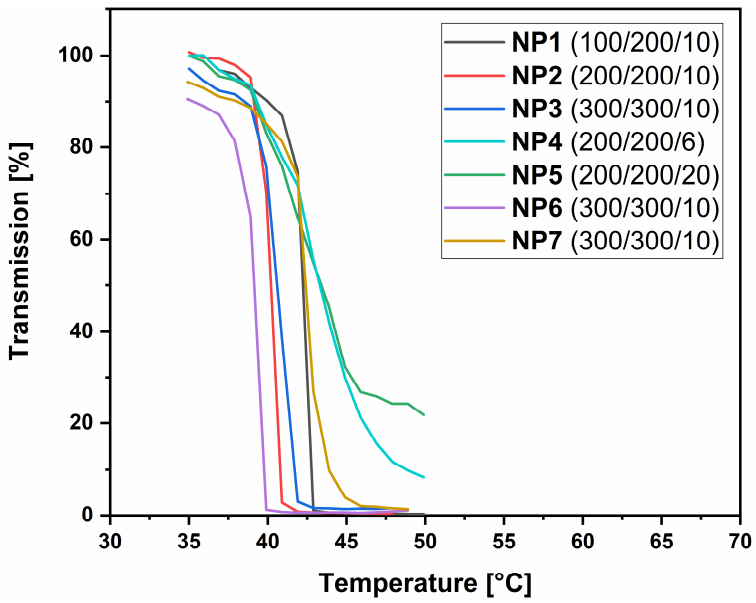

Fig. S42 Determination of the cloud points of the nanoparticles in aqueous solution (2.5 mg mL^{-1}).

Synthesis of the cysteamine-containing nanoparticles

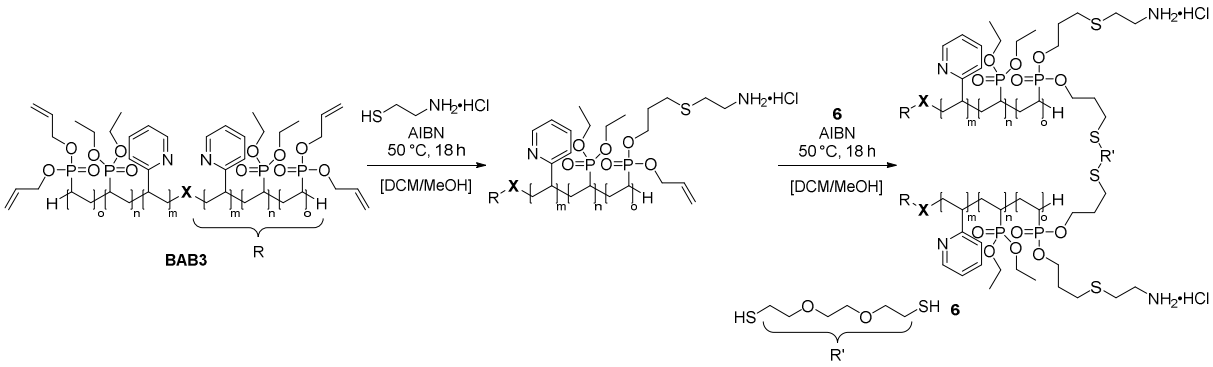

Copolymer **BAB3** (100 mg, 1.23 µmol) was dissolved in methylene chloride (20.0 mg) and treated with cysteamine-hydrochloride (980 µg, 8.62 µmol) in 2.00 mL methanol. After addition of catalytic amounts of AIBN, the solution was degassed, and stirred at 50 °C for 18 hours. The subsequent cross-linking was performed with dithiol **6** (4.90 mg, 26.9 µmol, 1.50 equiv. per allyl group). New AIBN was added and the reaction mixture was again stirred at 50 °C for 18 hours. The reaction progress was checked by proton NMR and after complete conversion of the allyl groups, the solvent was removed *in vacuo*, and the residue was dissolved in deionised water and purified by dialyses against water. Freeze-drying from water yielded the colourless solid (96.0 mg, 94 %).

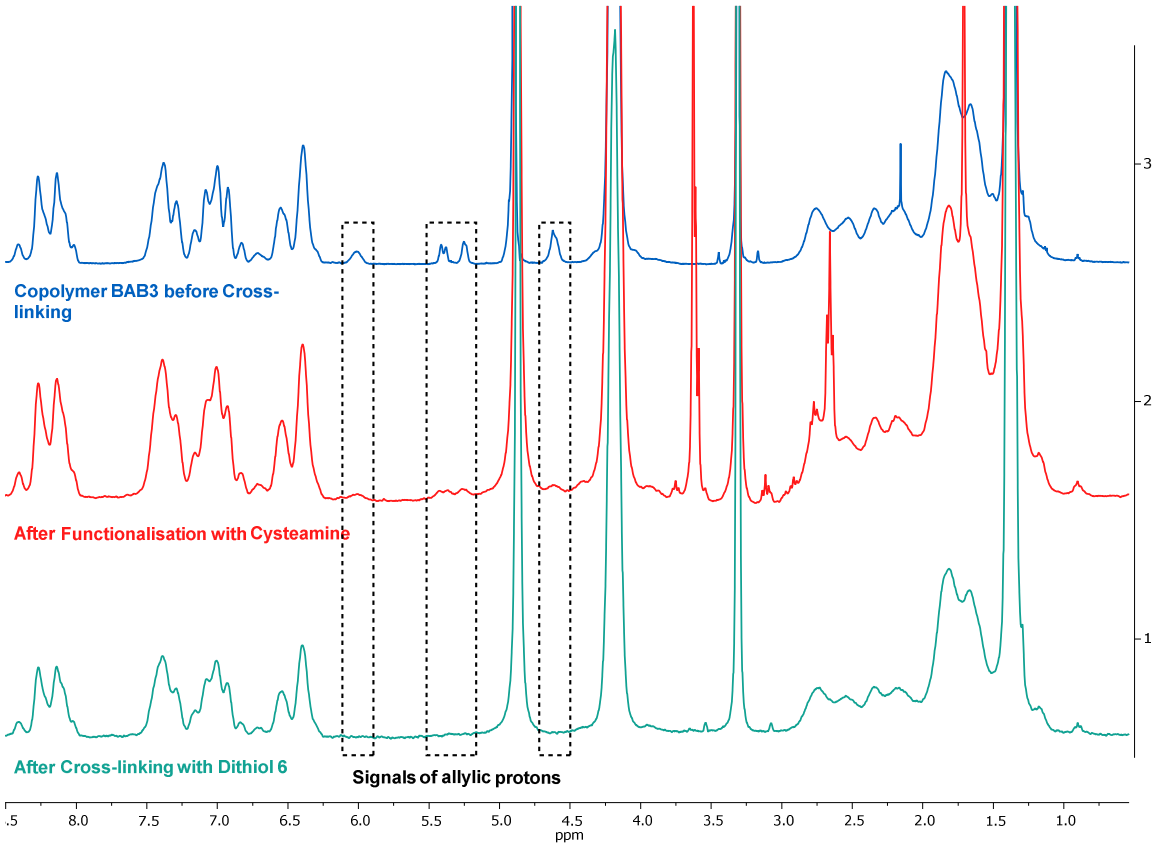

Fig. S43 Monitoring of the sequential functionalisation of **BAB3** (blue) with cysteamine-hydrochloride as linker unit (red) and cross-linking with dithiol **6** (turquoise) recorded in MeOD-d_4.

Conjugation of folate-NHS to the nanoparticle

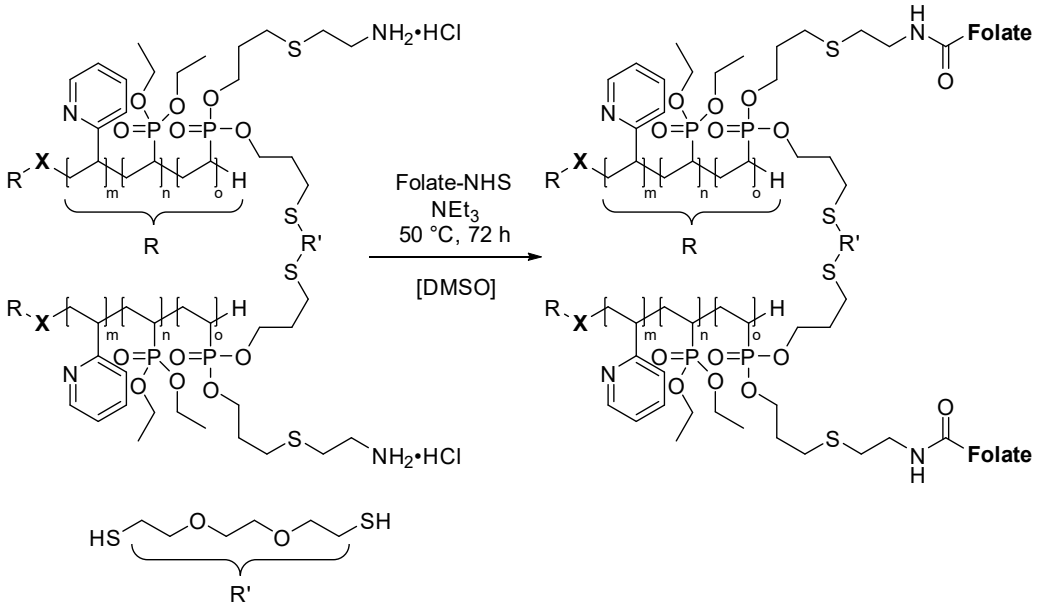

Folate-NHS (8.75 mg, 16.3 mg) and triethylamine (3.38 µL, 24.4 µmol) were added to a solution of the cysteamine-functionalised nanoparticles (96.0 mg, 1.16 µmol) in DMSO (20.0 mL). The solution was heated to 50°C and stirred for 72 hours. The reaction mixture was concentrated in high vacuum and purified by dialysis against water for 96 hours. The resulting, aqueous solution was lyophilised to yield the folate-containing substrate as a light-yellow solid (82.0 mg, 84 %).

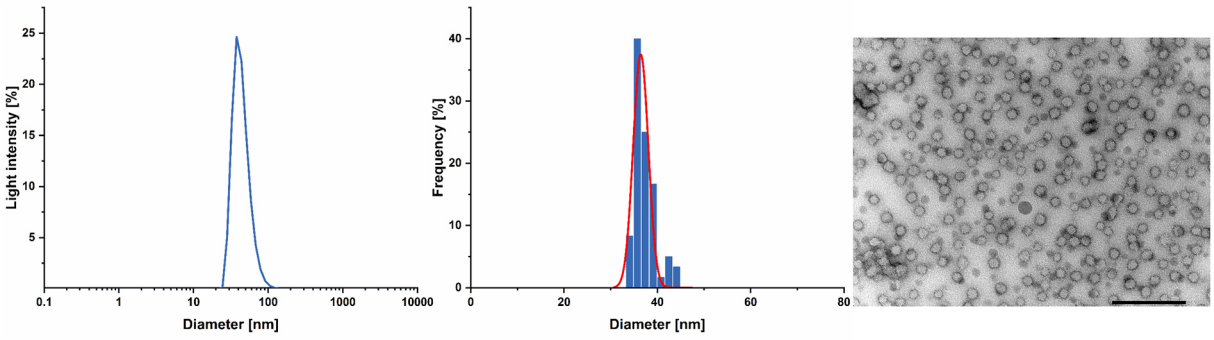

Fig. S44 Size distribution of the folate-functionalised nanoparticle ($2VP_{300}$-$DEVP_{300}$-$DAlVP_{10}$) determined *via* DLS measurements at a concentration of 2.5 mg mL^{-1} in *Millipore* water (left); histogram plot with a *gaussian* regression fit (middle); and a TEM image of folate-functionalised nanoparticle (right) with a scale bar of 200 nm.

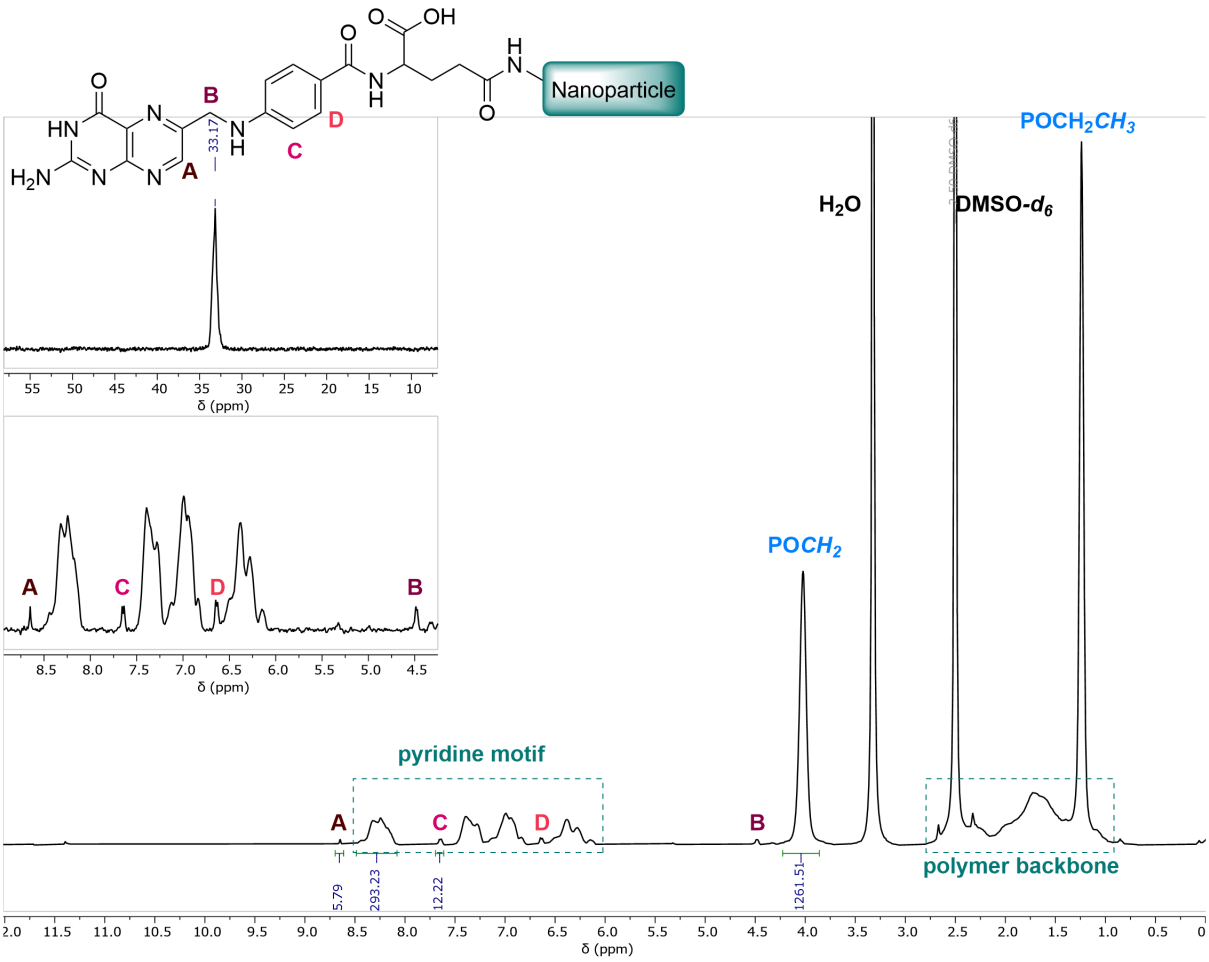

Fig. S45 ^{1}H- and ^{31}P-NMR of the folate functionalised nanoparticle recorded in DMSO-d_6. Detailed view on the region comprising folate corresponding signals between 4.25 and 8.90 ppm.

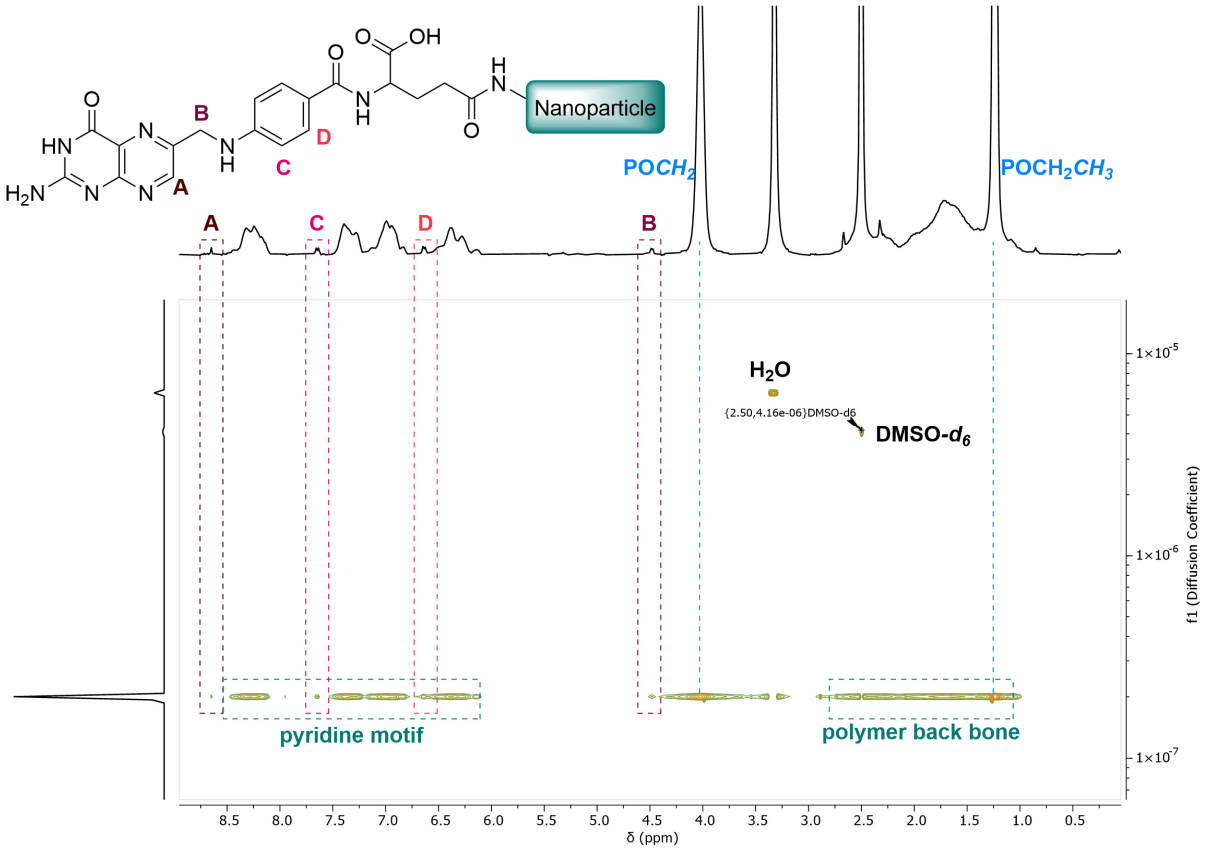

Fig. S46 DOSY-NMR of the folate functionalised nanoparticle recorded in DMSO-d_6.

8 References

1. K. C. Hultzsch, P. Voth, K. Beckerle, T. P. Spaniol and J. Okuda, *Organometallics*, 2000, **19**, 228-243.

2. G. D. Vaughn, K. A. Krein and J. A. Gladysz, *Organometallics*, 1986, **5**, 936-942.

3. C.-X. Cai, L. Toupet, C. W. Lehmann and J.-F. Carpentier, *J. Organomet. Chem.*, 2003, **683**, 131-136.

4. S. Salzinger, B. S. Soller, A. Plikhta, U. B. Seemann, E. Herdtweck and B. Rieger, *J. Am. Chem. Soc.*, 2013, **135**, 13030-13040.

5. B. S. Soller, S. Salzinger, C. Jandl, A. Pöthig and B. Rieger, *Organometallics*, 2015, **34**, 2703-2706.

6. M. Leute, DOI: 10.18725/OPARU-1106PhD, Universitity of Ulm, 2007.

7. C. Schwarzenböck, P. J. Nelson, R. Huss and B. Rieger, *Nanoscale*, 2018, **10**, 16062-16068.

8. L. Rigger, R. L. Schmidt, K. M. Holman, M. Simonović and R. Micura, *Chem. Eur. J.*, 2013, **19**, 15872-15878.

9. C. M. Alexander, K. L. Hamner, M. M. Maye and J. C. Dabrowiak, *Bioconjug. Chem.*, 2014, **25**, 1261-1271.

10. A. F. Trindade, R. F. M. Frade, E. M. S. Macoas, C. Graca, C. A. B. Rodrigues, J. M. G. Martinho and C. A. M. Afonso, *Org. Biomol. Chem.*, 2014, **12**, 3181-3190.